

614. Discontinuity and bifurcation analysis of motions in a fermi oscillator under dual excitations

Yu Guo and Albert C. J. Luo¹

Department of Mechanical and Industrial Engineering,
Southern Illinois University Edwardsville,
Edwardsville, IL 62026-1805, USA

Tel: (618) 650-5389

Fax: (618) 650-2555

E-mail: ¹*aluo@siue.edu*

(Received 02 November 2010; accepted 4 February 2011)

Abstract. In this paper, the stability and bifurcation of motions in a fermi oscillator under dual excitations are presented using the theory of discontinuous dynamical systems. The analytical conditions for motion switching in such a fermi-oscillator are obtained, and the generic mappings are introduced to describe the periodic and chaotic motions for such oscillator. Bifurcation scenarios for periodic and chaotic motions are presented together with analytical predictions of periodic motions. Finally, numerical illustrations of periodic and chaotic motions in such an oscillator are given. In addition, the flutter oscillations of such an oscillator are presented through the switching section for the Neimark bifurcation.

Keywords: Fermi oscillator, discontinuous dynamical systems, impacting chatter, sticking motion, Neimark bifurcation.

Introduction

The Fermi acceleration oscillator is a typical physical model, and such impact phenomena extensively exist in physics and engineering. In 1949, the Fermi acceleration was first introduced by Fermi [1] to explain the origin of cosmic radiation. In 1964, Zaslavskii and Chirikov [2] provided the criterion of the Fermi accelerator in one-dimensional case to explain chaotic motion existing. In 1982, Holmes [3] studied the dynamics of a ball impacting with an oscillating table. However, it was assumed that the mass of the ball is much smaller than the one of the table, and the impacts between the ball and tables are at the same position. In 1983, Shaw and Holmes [4] investigated the harmonic, sub-harmonic, and chaotic motions of a single-degree of freedom non-linear oscillator. Bapat and Popplewell [5] experimentally investigated the asymptotically stable periodic motions of a ball in an impact-pair. In 1988, Bapat [6] used the Fourier series and perturbation methods to determine the stability regions of two-equispaced-impact motion of a ball in an impact-pair. In 1995, Bapat [7] discussed the general motion of a ball in an inclined impact damper with friction. In 1996, Luo and Han [8] revisited the dynamics of a bouncing ball with a sinusoidal vibrating table. To further understand the nonlinear dynamical behaviors of the Fermi oscillator, in 1989, Luna-Acosta [9] investigated the dynamics of the Fermi accelerator with a viscous friction. In 1998, Lopac and Dananic [10] provided a further investigation of the chaotic dynamics and energy conservation in a

gravitationally driven Fermi accelerator, and Saif et al [11] discussed the classical and quantum dynamics of a Fermi accelerator and determined the existence of dynamical localization for both position and momentum in a window of the modulation amplitude. In 2004, Bouchet [12] presented a simple stochastic system to generate anomalous diffusion of both position and velocity for the Fermi accelerator. Leonel et al [13] used a discrete dynamical systems formalism to investigate the effect of a time-dependent perturbation on a Fermi accelerator model. In 2005, Leonel and McClintock [14] studied the dynamical and chaotic properties of a Fermi-Ulam bouncer model. In 2006, Leonel and Carvalho [15] used a two-dimensional nonlinear area-contracting map to study the Fermi accelerator model with inelastic collisions. In 2008, Leonel and Silva [16] studied the dynamical properties of a bouncing ball model with a nonlinear excitation force. The aforementioned studies did not consider the motion switchability and impact chatters, which cause the dynamical behavior complexity.

On the other hands, in 2002, Luo [17] discussed the stability and bifurcation analysis for the unsymmetrical periodic motion in a periodically excited horizontal impact oscillator. In 2004, Giusepponi et al [18] used the asynchronous sampling method to study the dynamical behaviors of a bouncing ball. In 2005, Luo [19] proposed the mapping dynamics method to determine periodic motion in a piecewise linear system. For a better understanding of such a kind of dynamical systems, Luo [20] developed a theory for the non-smooth dynamical systems on connectable and accessible sub-domains. Luo and Chen [21] used such a discontinuous dynamical system theory to investigate the flows and grazing bifurcations of an idealized gear transmission system with impacts. In 2006, Luo and Gegg [22] used such a theory to develop the force criteria for stick and non-stick motions in the friction-induced oscillator. In 2007, Luo and O'Connor [23, 24] studied the nonlinear dynamics of a gear transmission system through an impact model with possible stick. Luo and Guo [25-27] systematically investigated the switching bifurcation and chaos in a generalized Fermi oscillator accelerated with a simple excitation. Under dual excitations, the complexity of chaos and periodic motions for the particles in the Fermi oscillators will be different from the single excitation. Thus, in Luo and Guo [28], the initial studies were completed.

In this paper, motion complexity in the Fermi oscillator with dual excitations will be investigated. The analytical conditions for switchability of the motions in such a system will be developed. Generic mappings will be introduced to describe different types of motions in such oscillators. Analytical predictions of periodic motions will then be presented through the mapping structures. Finally, periodic and chaotic motions in such an oscillator will be simulated, and Poincare mappings for the Neimark bifurcation will be presented as well.

Physical model

As in Luo and Guo [28], the Fermi accelerator with dual excitations consists of a particle moving vertically between two periodically excited oscillators. The mass in each oscillator $m^{(\alpha)}$ ($\alpha \in \{1, 2\}$) is connected with a spring of constant $k^{(\alpha)}$ and a damper of coefficient $c^{(\alpha)}$ to the fixed wall. Both oscillators are driven with periodic excitation force $F^{(\alpha)}(t)$, as shown in Figure 1. The mass of particle is $m^{(3)}$ and the restitution coefficients of impact for the bottom and top oscillators are $e^{(1)}$ and $e^{(2)}$, respectively. The gap between the equilibrium positions of the two oscillators is h . If the particle does not move together with any of the oscillators, the corresponding motion is called the non-stick motion. For this case, the equations of motion are given by the Newton's law, i.e.,

$$\left. \begin{aligned} \ddot{x}^{(3)} &= -g, \\ \ddot{x}^{(\alpha)} + 2\xi^{(\alpha)}\dot{x}^{(\alpha)} + (\omega^{(\alpha)})^2 x^{(\alpha)} &= \frac{Q^{(\alpha)}}{m^{(\alpha)}} \cos \Omega^{(\alpha)} t, \end{aligned} \right\} \quad (1)$$

where $\xi^{(\alpha)} = c^{(\alpha)} / 2m^{(\alpha)}$, $\omega^{(\alpha)} = \sqrt{k^{(\alpha)} / m^{(\alpha)}}$. $\ddot{x}^{(i)}$ is the acceleration, $\dot{x}^{(i)}$ is the velocity, and $x^{(i)}$ is the displacement ($i = 1, 2, 3$).

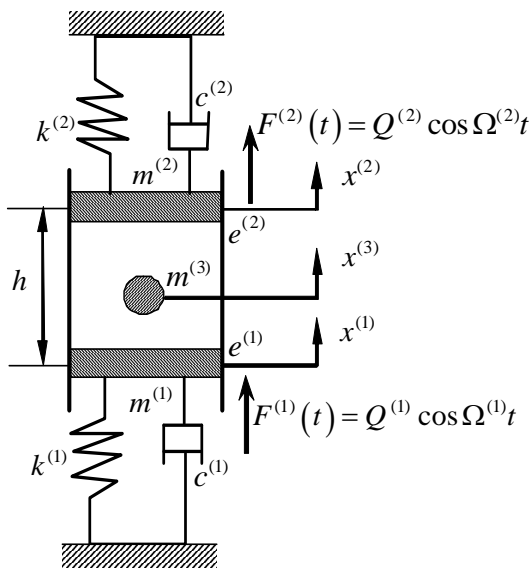


Fig. 1. Mechanical model

If the particle stays on one of the two oscillators and moves together, this motion is called a stick motion. For this case, the equations of motion are given as

$$\left. \begin{aligned} \ddot{x}^{(\alpha)} + 2\xi^{(\alpha)}\dot{x}^{(\alpha)} + (\omega^{(\alpha)})^2 x^{(\alpha)} &= \frac{Q^{(\alpha)}}{m^{(\alpha)}} \cos \Omega^{(\alpha)} t, \\ \ddot{x}^{(0)} + 2d^{(0)}\dot{x}^{(0)} + (\omega^{(0)})^2 x^{(0)} &= \frac{Q^{(\bar{\alpha})}}{m^{(3)} + m^{(\bar{\alpha})}} \cos \Omega^{(\bar{\alpha})} t, \end{aligned} \right\} \quad (2)$$

where $\ddot{x}^{(0)}$ is the acceleration, $\dot{x}^{(0)}$ is the velocity, and $x^{(0)}$ is the displacement for both the ball and oscillator. Also $d^{(0)} = c^{(\bar{\alpha})} / 2(m^{(3)} + m^{(\bar{\alpha})})$, $\omega^{(0)} = \sqrt{k^{(\bar{\alpha})} / m^{(3)} + m^{(\bar{\alpha})}}$ where

$$\bar{\alpha} = \begin{cases} 2, & \text{if } \alpha = 1; \\ 1, & \text{if } \alpha = 2. \end{cases} \quad (3)$$

The impact relations among the particle and the oscillators are

$$\begin{aligned} x_+^{(3)} &= x_+^{(\alpha)} = x_-^{(3)} = x_-^{(\alpha)}; \\ \dot{x}_+^{(3)} &= \frac{m^{(3)}\dot{x}_-^{(3)} + m^{(\alpha)}\dot{x}_-^{(\alpha)} - m^{(\alpha)}e^{(\alpha)}(\dot{x}_-^{(3)} - \dot{x}_-^{(\alpha)})}{m^{(3)} + m^{(\alpha)}}, \\ \dot{x}_+^{(\alpha)} &= \frac{m^{(3)}\dot{x}_-^{(3)} + m_2\dot{x}_-^{(\alpha)} + m^{(3)}e^{(\alpha)}(\dot{x}_-^{(3)} - \dot{x}_-^{(\alpha)})}{m^{(3)} + m^{(\alpha)}}. \end{aligned} \quad (4)$$

Discontinuous descriptions

Due to the discontinuity of the system, the domains and boundaries in absolute coordinate system are introduced as sketched in Figure 2. The origin of the absolute coordinate is set at the equilibrium position of the bottom oscillator. The absolute domains $\Omega_1^{(1)}$ and $\Omega_1^{(2)}$ for the bottom and top oscillators and domain $\Omega_1^{(3)}$ for the particle without stick are defined as

$$\left. \begin{aligned} \Omega_1^{(1)} &= \{(x^{(1)}, \dot{x}^{(1)}) \mid x^{(1)} \in (-\infty, x^{(3)})\}, \\ \Omega_1^{(2)} &= \{(x^{(2)}, \dot{x}^{(2)}) \mid x^{(2)} \in (x^{(3)}, +\infty)\}, \\ \Omega_1^{(3)} &= \{(x^{(3)}, \dot{x}^{(3)}) \mid x^{(3)} \in (x^{(1)}, x^{(2)})\}. \end{aligned} \right\} \quad (5)$$

The corresponding absolute boundaries are defined as

$$\left. \begin{aligned} \partial\Omega_{1(+\infty)}^{(i)} &= \{(x^{(i)}, \dot{x}^{(i)}) \mid \varphi_{1(+\infty)}^{(i)} \equiv x^{(i)} - x^{(\bar{i})} = 0, \dot{x}^{(i)} \neq \dot{x}^{(\bar{i})}\}, \\ \partial\Omega_{1(-\infty)}^{(j)} &= \{(x^{(j)}, \dot{x}^{(j)}) \mid \varphi_{1(-\infty)}^{(j)} \equiv x^{(j)} - x^{(\bar{j})} = 0, \dot{x}^{(j)} \neq \dot{x}^{(\bar{j})}\}, \end{aligned} \right\} \quad (6)$$

where $i = 2, 3$ and $\bar{i} = 3, 2$ with $(j = 1, 3$ and $\bar{j} = 3, 1)$. The domains are represented by a shaded area and the boundaries are depicted by dashed and solid curves in Figure 2. The boundaries of $\partial\Omega_{1(+\infty)}^{(2)}$ and $\partial\Omega_{1(+\infty)}^{(3)}$ are the curves at $x^{(2)} = x^{(3)}$ and the boundaries of $\partial\Omega_{1(-\infty)}^{(1)}$ and $\partial\Omega_{1(-\infty)}^{(3)}$ are the curves at $x^{(1)} = x^{(2)}$. For stick motion, the absolute domains $\Omega_0^{(i)}$ and $\Omega_1^{(i)}$ ($i = 1, 2, 3$) for the two oscillators and particle are defined as

$$\left. \begin{aligned}
 \Omega_0^{(1)} &= \left\{ (x^{(1)}, \dot{x}^{(1)}) \mid x^{(1)} \in (x_{cr}^{(3)}, x^{(2)}), \dot{x}^{(1)} = \dot{x}^{(3)} \right\}, \\
 \Omega_0^{(2)} &= \left\{ (x^{(2)}, \dot{x}^{(2)}) \mid x^{(2)} \in (x^{(1)}, x_{cr}^{(3)}), \dot{x}^{(2)} = \dot{x}^{(3)} \right\}, \\
 \Omega_0^{(3)} &= \left\{ (x^{(3)}, \dot{x}^{(3)}) \mid \begin{array}{l} x^{(3)} \in (-\infty, x_{cr}^{(1)}), \dot{x}^{(3)} = \dot{x}^{(1)} \\ \text{OR } x^{(3)} \in (x_{cr}^{(2)}, +\infty), \dot{x}^{(3)} = \dot{x}^{(2)} \end{array} \right\}, \\
 \Omega_1^{(1)} &= \left\{ (x^{(1)}, \dot{x}^{(1)}) \mid x^{(1)} \in (-\infty, x_{cr}^{(3)}), \dot{x}^{(3)} \neq \dot{x}^{(1)} \right\}, \\
 \Omega_1^{(2)} &= \left\{ (x^{(2)}, \dot{x}^{(2)}) \mid x^{(2)} \in (x_{cr}^{(3)}, +\infty), \dot{x}^{(3)} \neq \dot{x}^{(2)} \right\}, \\
 \Omega_1^{(3)} &= \left\{ (x^{(3)}, \dot{x}^{(3)}) \mid \begin{array}{l} x^{(3)} \in (x_{cr}^{(1)}, x^{(2)}), \dot{x}^{(3)} \neq \dot{x}^{(1)} \\ \text{OR } x^{(3)} \in (x^{(1)}, x_{cr}^{(2)}), \dot{x}^{(3)} \neq \dot{x}^{(2)} \end{array} \right\},
 \end{aligned} \right\} \quad (7)$$

where $x_{cr}^{(i)}$ is for appearance and vanishing of stick motion with $\dot{x}_{cr}^{(3)} = \dot{x}_{cr}^{(\alpha)}$ and $x_{cr}^{(3)} = x_{cr}^{(a)}$, and $\alpha = 1, 2$ are for stick on the bottom and top, respectively. The domains of $\Omega_1^{(i)}$ and $\Omega_0^{(i)}$ are presented by shaded and filled regions in Figure 3. The corresponding absolute boundaries are given by dashed curves, and the stick boundaries are defined as

$$\left. \begin{aligned}
 \partial\Omega_{10}^{(1)} &= \left\{ (x^{(1)}, \dot{x}^{(1)}) \mid \varphi_{10}^{(1)} \equiv x^{(1)} - x_{cr}^{(3)} = 0, \dot{x}^{(1)} = \dot{x}_{cr}^{(3)} \right\}, \\
 \partial\Omega_{10}^{(2)} &= \left\{ (x^{(2)}, \dot{x}^{(2)}) \mid \varphi_{10}^{(2)} \equiv x^{(2)} - x_{cr}^{(3)} = 0, \dot{x}^{(2)} = \dot{x}_{cr}^{(3)} \right\}, \\
 \partial\Omega_{10}^{(3)} &= \left\{ (x^{(3)}, \dot{x}^{(3)}) \mid \begin{array}{l} \varphi_{10}^{(3)} \equiv x^{(3)} - x_{cr}^{(1)} = 0, \dot{x}^{(3)} = \dot{x}_{cr}^{(1)} \\ \text{OR } \varphi_{10}^{(3)} \equiv x^{(3)} - x_{cr}^{(2)} = 0, \dot{x}^{(3)} = \dot{x}_{cr}^{(2)} \end{array} \right\}.
 \end{aligned} \right\} \quad (8)$$

The vectors for absolute motions can be defined as follows

$$\left. \begin{aligned}
 \mathbf{x}_\lambda^{(i)} &= (x_\lambda^{(i)}, \dot{x}_\lambda^{(i)})^T, \\
 \mathbf{f}_\lambda^{(i)} &= (\dot{x}_\lambda^{(i)}, F_\lambda^{(i)})^T,
 \end{aligned} \right\} \text{ for } (i = 1, 2, 3 \text{ and } \lambda = 0, 1), \quad (9)$$

where $i = 1, 2, 3$ represents the bottom, top oscillators, and the particle, respectively; $\lambda = 0, 1$ stands for the stick or non-stick domains. Then equation of absolute motion is

$$\dot{\mathbf{x}}_\lambda^{(i)} = \mathbf{f}_\lambda^{(i)}(\mathbf{x}_\lambda^{(i)}, t) \quad \text{for } i = 1, 2, 3 \text{ and } \lambda = 0, 1. \quad (10)$$

For non-stick motion,

$$\left. \begin{aligned}
 F_1^{(i)}(x_1^{(i)}, t) &= -2\xi^{(i)}\dot{x}^{(i)} - (\omega^{(i)})^2 x^{(i)} + \frac{Q^{(i)}}{m^{(i)}} \cos \Omega^{(i)} t, \quad (i = 1, 2), \\
 F_1^{(3)}(x_1^{(3)}, t) &= -g.
 \end{aligned} \right\} \quad (11)$$

For the stick motion,

$$\left. \begin{aligned} F_1^{(\bar{\alpha})}(x_1^{(\bar{\alpha})}, t) &= -2\xi^{(\bar{\alpha})}\dot{x}^{(\bar{\alpha})} - (\omega^{(\bar{\alpha})})^2 x^{(\bar{\alpha})} + \frac{Q^{(\bar{\alpha})}}{m^{(\bar{\alpha})}} \cos \Omega^{(\bar{\alpha})} t \\ F_0^{(i)}(x_0^{(i)}, t) &= -2d^{(0)}\dot{x}^{(0)} - (\omega^{(0)})^2 x^{(0)} + \frac{Q^{(\alpha)}}{m^{(3)} + m^{(\alpha)}} \cos \Omega^{(\alpha)} t \end{aligned} \right\} (i = \alpha, 3). \quad (12)$$

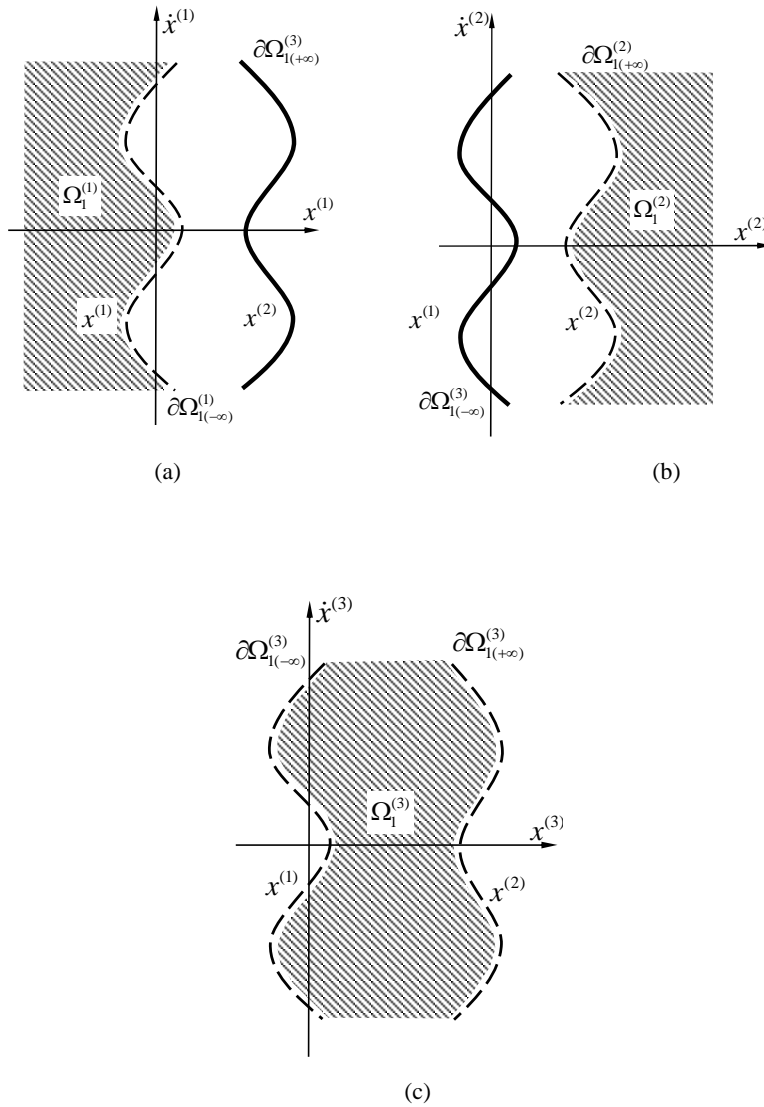


Fig. 2. Absolute domains and boundaries without stick: (a) bottom oscillator, (b) top oscillator, and (c) particle

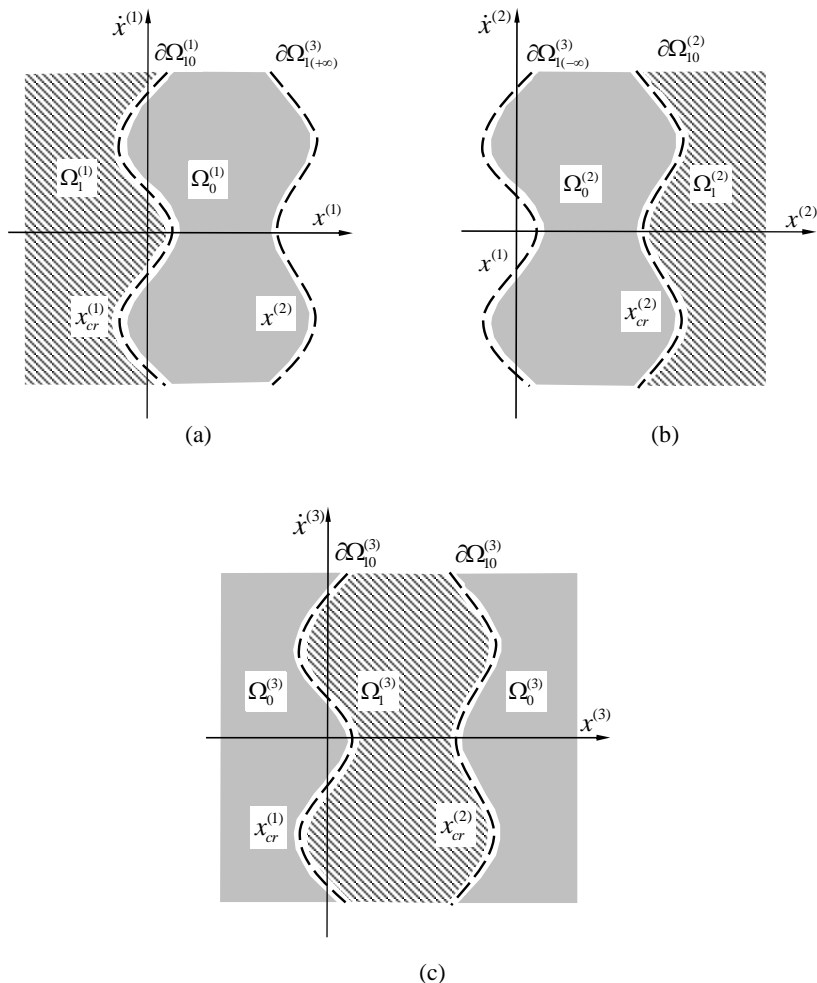


Fig. 3. Absolute domains and boundaries with stick: (a) bottom oscillator, (b) top oscillator, and (c) particle

For simplicity, the relative displacement, velocity, and acceleration between the particle and the bottom or top oscillators are defined as $z^{(i)} = x^{(i)} - x^{(\bar{i})}$, $\dot{z}^{(i)} = \dot{x}^{(i)} - \dot{x}^{(\bar{i})}$, and $\ddot{z}^{(i)} = \ddot{x}^{(i)} - \ddot{x}^{(\bar{i})}$, where $i = \alpha, 3$ and $\bar{i} = 3, \alpha$ represent the particle and one of the two oscillators, accordingly. The relative domains and boundaries for the particle and oscillators are then defined as sketched in Figure 4 and Figure 5 for the motion relative to bottom or top oscillators. The stick domain and boundaries in the relative phase space becomes a point in Figure 4 and Figure 5(a) and (c). Therefore, the stick domains and boundaries in the relative velocity and acceleration (i.e., $(\dot{z}^{(i)}, \ddot{z}^{(i)})$) plane are presented in Figure 4 and Figure 5(b) and (d).

The filled regions represent the stick motion domains while the shaded regions indicate the non-stick motion domains. The domains $\Omega_0^{(i)}$ and $\Omega_1^{(i)}$ for the relative motions for the particle and the two oscillators are

$$\left. \begin{aligned}
 \Omega_0^{(i)} &= \left\{ (z^{(i)}, \dot{z}^{(i)}) \mid \dot{z}^{(i)} = 0, z^{(i)} = 0 \right\}, \\
 \Omega_1^{(1)} &= \left\{ (z^{(1)}, \dot{z}^{(1)}) \mid z^{(1)} \in (-\infty, 0) \right\}, \\
 \Omega_1^{(2)} &= \left\{ (z^{(2)}, \dot{z}^{(2)}) \mid z^{(2)} \in (0, +\infty) \right\}, \\
 \Omega_1^{(3)} &= \left\{ (z^{(3)}, \dot{z}^{(3)}) \mid z^{(3)} \in (x^{(1)} - x^{(3)}, 0), \right. \\
 &\quad \left. \text{or } z^{(3)} \in (0, x^{(2)} - x^{(3)}) \right\}.
 \end{aligned} \right\} \quad (13)$$

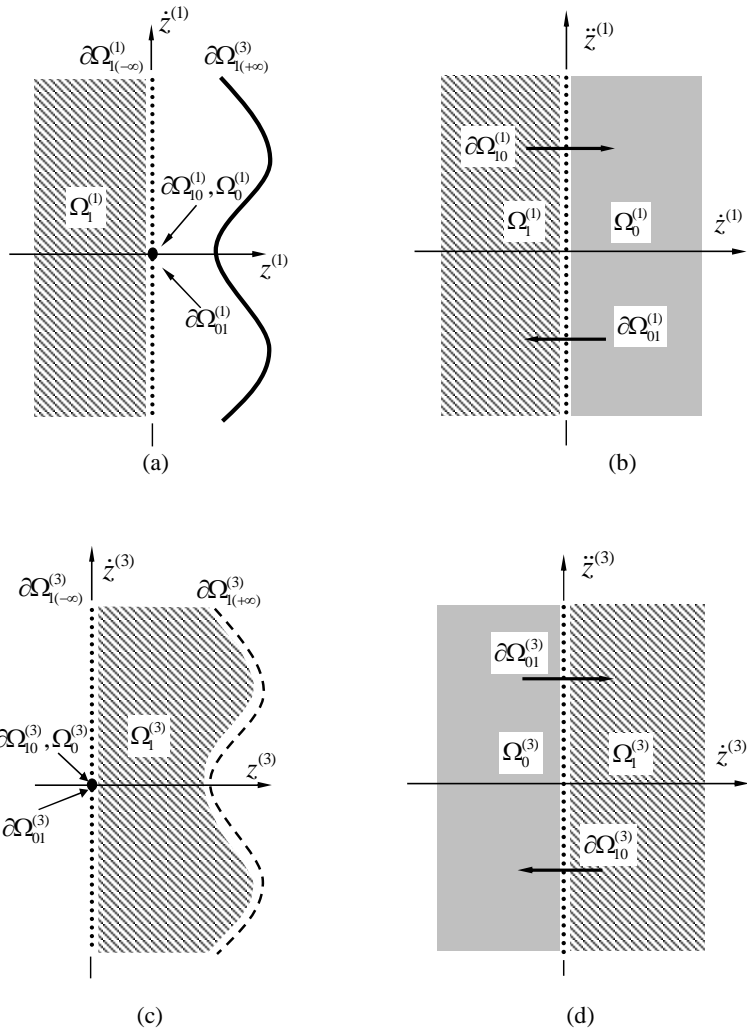


Fig. 4. Domains and boundaries definition relative to the bottom oscillator: (a) (z, \dot{z}) -plane for bottom oscillator, (b) (\dot{z}, \ddot{z}) -plane for bottom oscillator, (c) (z, \dot{z}) -plane for particle, and (d) (\dot{z}, \ddot{z}) -plane for particle

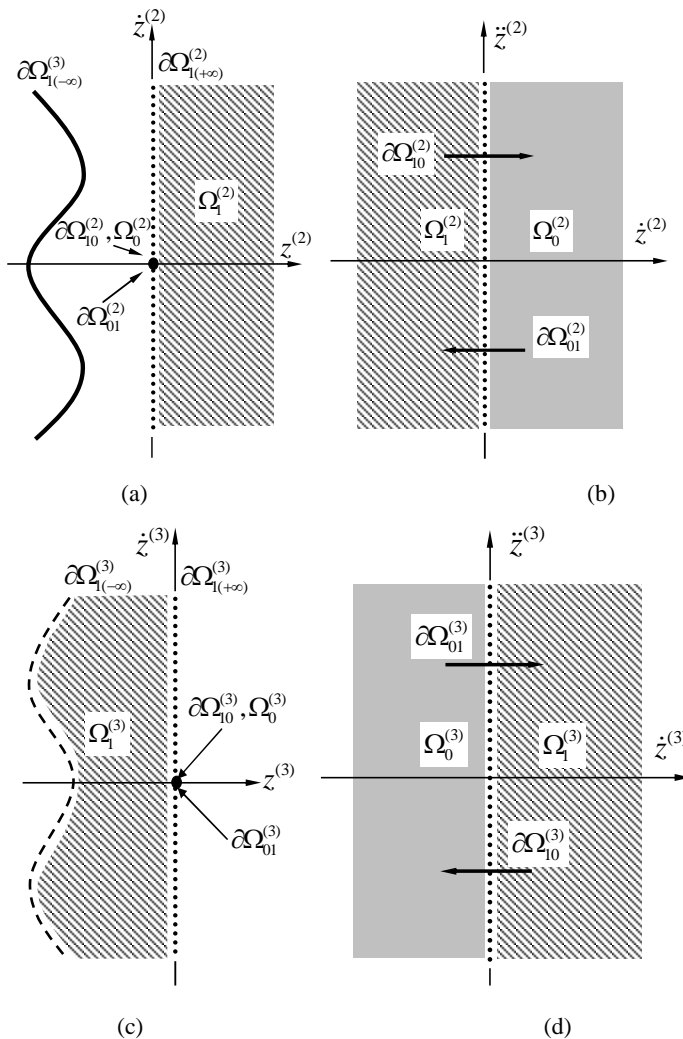


Fig. 5. Domains and boundaries definition relative to the top oscillator: (a) (z, \dot{z}) -plane for top oscillator, (b) (\dot{z}, \ddot{z}) -plane for top oscillator, (c) (z, \dot{z}) -plane for particle, and (d) (\dot{z}, \ddot{z}) -plane for particle

The boundaries $\partial\Omega_{1(+\infty)}^{(i)}$, $\partial\Omega_{1(-\infty)}^{(i)}$, $\partial\Omega_{10}^{(i)}$, and $\partial\Omega_{01}^{(i)}$ for the particle associated with the bottom or top oscillators are

$$\left. \begin{aligned} \partial\Omega_{1(-\infty)}^{(i)} &= \{(z^{(i)}, \dot{z}^{(i)}) \mid \varphi_{1(-\infty)}^{(i)} \equiv z^{(i)} = 0, \dot{z}^{(i)} \neq 0\}, \\ \partial\Omega_{1(+\infty)}^{(j)} &= \{(z^{(j)}, \dot{z}^{(j)}) \mid \varphi_{1(+\infty)}^{(j)} \equiv z^{(j)} = 0, \dot{z}^{(j)} \neq 0\}, \\ \partial\Omega_{10}^{(l)} &= \partial\Omega_{01}^{(l)} = \{(z^{(l)}, \dot{z}^{(l)}) \mid \varphi_{10}^{(l)} \equiv \dot{z}_{cr}^{(l)} = 0, z_{cr}^{(l)} = 0\}, \end{aligned} \right\} \quad (14)$$

where $i = 1, 3, j = 2, 3, l = 1, 2, 3$. $\partial\Omega_{1(-\infty)}^{(3)}$ and $\partial\Omega_{1(+\infty)}^{(3)}$ are the impact chatter boundaries for the particle relative to the bottom or top oscillators, respectively. $\partial\Omega_{10}^{(3)}$ and $\partial\Omega_{01}^{(3)}$ are the stick motion boundaries for the particle. $\partial\Omega_{1(-\infty)}^{(1)}$ and $\partial\Omega_{1(+\infty)}^{(2)}$ are the impact-chatter boundaries for the bottom or top oscillators, respectively. $\partial\Omega_{10}^{(1)}$ and $\partial\Omega_{01}^{(1)}$ are the stick motion boundaries for the bottom oscillator. $\partial\Omega_{10}^{(2)}$ and $\partial\Omega_{01}^{(2)}$ are the stick motion boundaries for the top oscillator. The relative vectors in the relative coordinates are

$$\mathbf{z}_\lambda^{(i)} = (z_\lambda^{(i)}, \dot{z}_\lambda^{(i)})^T, \mathbf{g}_\lambda^{(i)} = \dot{\mathbf{z}}_\lambda^{(i)} = (\dot{z}_\lambda^{(i)}, g_\lambda^{(i)})^T, \quad (15)$$

where $i = 1, 2$ are the bottom and top oscillators, respectively; $i = 3$ are for the particle. $\lambda = 0, 1$ gives the corresponding stick and non-stick domains. For $i = 1, 2, 3$ and $\lambda = 0, 1$, the equations of relative motion are in the relative vector form of

$$\left. \begin{aligned} \dot{\mathbf{z}}_\lambda^{(\bar{\alpha})} &= \mathbf{g}_\lambda^{(\bar{\alpha})}(\mathbf{x}_\lambda^{(\bar{\alpha})}, t), \\ \dot{\mathbf{z}}_\lambda^{(\alpha)} &= \mathbf{g}_\lambda^{(\alpha)}(\mathbf{z}_\lambda^{(\alpha)}, \mathbf{x}_\lambda^{(3)}, t), \\ \dot{\mathbf{z}}_\lambda^{(3)} &= \mathbf{g}_\lambda^{(3)}(\mathbf{z}_\lambda^{(3)}, \mathbf{x}_\lambda^{(\alpha)}, t), \end{aligned} \right\} \quad (16)$$

where $\dot{\mathbf{x}}_\lambda^{(i)} = \mathbf{f}_\lambda^{(i)}(\mathbf{x}_\lambda^{(i)}, t)$.

(i) For non-stick motion, the relative forces per unit mass are

$$\left. \begin{aligned} g_1^{(\bar{\alpha})}(\mathbf{z}_1^{(\bar{\alpha})}, \mathbf{x}_1^{(\bar{\alpha})}, t) &= -2\xi^{(\bar{\alpha})}\dot{x}_1^{(\bar{\alpha})} - (\omega^{(\bar{\alpha})})^2 x_1^{(\bar{\alpha})} + \frac{Q^{(\bar{\alpha})}}{m^{(\bar{\alpha})}} \cos \Omega^{(\bar{\alpha})} t, \\ g_1^{(\alpha)}(\mathbf{z}_1^{(\alpha)}, \mathbf{x}_1^{(\alpha)}, t) &= -2\xi^{(\alpha)}\dot{x}_1^{(\alpha)} - (\omega^{(\alpha)})^2 x_1^{(\alpha)} + \frac{Q^{(\alpha)}}{m^{(\alpha)}} \cos \Omega^{(\alpha)} t + g, \\ g_1^{(3)}(\mathbf{z}_1^{(3)}, \mathbf{x}_1^{(\alpha)}, t) &= -g + 2\xi^{(\alpha)}\dot{x}_1^{(\alpha)} + (\omega^{(\alpha)})^2 x_1^{(\alpha)} - \frac{Q^{(\alpha)}}{m^{(\alpha)}} \cos \Omega^{(\alpha)} t, \end{aligned} \right\} \quad (17)$$

(ii) For stick motion, the relative velocities and the relative forces per unit mass are

$$\left. \begin{aligned} \dot{z}_0^{(3)} &= \dot{z}_0^{(\alpha)} = 0, \\ g_1^{(\bar{\alpha})}(\mathbf{z}_1^{(\bar{\alpha})}, \mathbf{x}_1^{(\bar{\alpha})}, t) &= -2\xi^{(\bar{\alpha})}\dot{x}_1^{(\bar{\alpha})} - (\omega^{(\bar{\alpha})})^2 x_1^{(\bar{\alpha})} + \frac{Q^{(\bar{\alpha})}}{m^{(\bar{\alpha})}} \cos \Omega^{(\bar{\alpha})} t, \\ g_0^{(\alpha)}(\mathbf{z}_1^{(\alpha)}, \mathbf{x}_1^{(\alpha)}, t) &= g_0^{(3)}(\mathbf{z}_1^{(3)}, \mathbf{x}_1^{(\alpha)}, t) = 0. \end{aligned} \right\} \quad (18)$$

Mathematical conditions of switchability

To develop the analytical conditions for stick and grazing motions of the Fermi oscillator, the normal vector of the boundary relative to the bottom or top oscillator is

$$\mathbf{n}_{\partial\Omega_{\alpha\beta}} = \nabla \varphi_{\alpha\beta} = \left(\frac{\partial \varphi_{\alpha\beta}}{\partial z}, \frac{\partial \varphi_{\alpha\beta}}{\partial \dot{z}} \right)^T, \quad (19)$$

where $\nabla = (\partial/\partial z, \partial/\partial \dot{z})^T$. $\mathbf{n}_{\partial\Omega_{10}^{(3)}}$ and $\mathbf{n}_{\partial\Omega_{01}^{(3)}}$ are the normal vectors of the stick boundaries, and the normal vectors of $\mathbf{n}_{\partial\Omega_{1(-\infty)}^{(3)}}$ and $\mathbf{n}_{\partial\Omega_{1(+\infty)}^{(3)}}$ are for impact chatter boundaries. Thus,

$$\left. \begin{aligned} \mathbf{n}_{\partial\Omega_{10}^{(3)}} = \mathbf{n}_{\partial\Omega_{01}^{(3)}} &= (0, 1)^T, \\ \mathbf{n}_{\partial\Omega_{1(-\infty)}^{(3)}} = \mathbf{n}_{\partial\Omega_{1(+\infty)}^{(3)}} &= (1, 0)^T. \end{aligned} \right\} \quad (20)$$

Zero-order and first-order G-functions for the stick boundaries relative to the bottom or top oscillators are introduced from Luo [29, 30],

$$\left. \begin{aligned} G_{\partial\Omega_{01}^{(\alpha)}}^{(0,0)}(\mathbf{z}_0^{(\alpha)}, \mathbf{x}_0^{(3)}, t_{m\pm}) &= \mathbf{n}_{\partial\Omega_{01}^{(\alpha)}}^T \cdot \mathbf{g}^{(\alpha)}(\mathbf{z}_0^{(\alpha)}, \mathbf{x}_0^{(3)}, t_{m\pm}), \\ G_{\partial\Omega_{10}^{(\alpha)}}^{(1,0)}(\mathbf{z}_1^{(\alpha)}, \mathbf{x}_1^{(3)}, t_{m\pm}) &= \mathbf{n}_{\partial\Omega_{10}^{(\alpha)}}^T \cdot \mathbf{g}^{(\alpha)}(\mathbf{z}_1^{(\alpha)}, \mathbf{x}_1^{(3)}, t_{m\pm}), \\ G_{\partial\Omega_{01}^{(\alpha)}}^{(0,1)}(\mathbf{z}_0^{(\alpha)}, \mathbf{x}_0^{(3)}, t_{m\pm}) &= \mathbf{n}_{\partial\Omega_{01}^{(\alpha)}}^T \cdot D\mathbf{g}^{(\alpha)}(\mathbf{z}_0^{(\alpha)}, \mathbf{x}_0^{(3)}, t_{m\pm}), \\ G_{\partial\Omega_{10}^{(\alpha)}}^{(1,1)}(\mathbf{z}_1^{(\alpha)}, \mathbf{x}_1^{(3)}, t_{m\pm}) &= \mathbf{n}_{\partial\Omega_{10}^{(\alpha)}}^T \cdot D\mathbf{g}^{(\alpha)}(\mathbf{z}_1^{(\alpha)}, \mathbf{x}_1^{(3)}, t_{m\pm}), \\ G_{\partial\Omega_{01}^{(3)}}^{(0,0)}(\mathbf{z}_0^{(3)}, \mathbf{x}_0^{(\alpha)}, t_{m\pm}) &= \mathbf{n}_{\partial\Omega_{01}^{(3)}}^T \cdot \mathbf{g}^{(3)}(\mathbf{z}_0^{(3)}, \mathbf{x}_0^{(\alpha)}, t_{m\pm}), \\ G_{\partial\Omega_{10}^{(3)}}^{(1,0)}(\mathbf{z}_1^{(3)}, \mathbf{x}_1^{(\alpha)}, t_{m\pm}) &= \mathbf{n}_{\partial\Omega_{10}^{(3)}}^T \cdot \mathbf{g}^{(3)}(\mathbf{z}_1^{(3)}, \mathbf{x}_1^{(\alpha)}, t_{m\pm}), \\ G_{\partial\Omega_{01}^{(3)}}^{(0,1)}(\mathbf{z}_0^{(3)}, \mathbf{x}_0^{(\alpha)}, t_{m\pm}) &= \mathbf{n}_{\partial\Omega_{01}^{(3)}}^T \cdot D\mathbf{g}^{(3)}(\mathbf{z}_0^{(3)}, \mathbf{x}_0^{(\alpha)}, t_{m\pm}), \\ G_{\partial\Omega_{10}^{(3)}}^{(1,0)}(\mathbf{z}_1^{(3)}, \mathbf{x}_1^{(\alpha)}, t_{m\pm}) &= \mathbf{n}_{\partial\Omega_{10}^{(3)}}^T \cdot D\mathbf{g}^{(3)}(\mathbf{z}_1^{(3)}, \mathbf{x}_1^{(\alpha)}, t_{m\pm}). \end{aligned} \right\} \quad (21)$$

Notice that t_m is the switching time of the motion on the corresponding boundary and $t_{m\pm} = t_m \pm 0$, which represents the motion on each side of the boundary in different domains. The G-functions for the impact chatter boundaries are

$$\left. \begin{aligned} G_{\partial\Omega_{1(+\infty)}^{(3)}}^{(0,1)}(\mathbf{z}_1^{(3)}, \mathbf{x}_1^{(2)}, t_{m\pm}) &= \mathbf{n}_{\partial\Omega_{1(+\infty)}^{(3)}}^T \cdot \mathbf{g}^{(3)}(\mathbf{z}_1^{(3)}, \mathbf{x}_1^{(2)}, t_{m\pm}), \\ G_{\partial\Omega_{1(+\infty)}^{(3)}}^{(1,1)}(\mathbf{z}_1^{(3)}, \mathbf{x}_1^{(2)}, t_{m\pm}) &= \mathbf{n}_{\partial\Omega_{1(+\infty)}^{(3)}}^T \cdot D\mathbf{g}^{(3)}(\mathbf{z}_1^{(3)}, \mathbf{x}_1^{(2)}, t_{m\pm}), \\ G_{\partial\Omega_{1(-\infty)}^{(3)}}^{(0,1)}(\mathbf{z}_1^{(3)}, \mathbf{x}_1^{(1)}, t_{m\pm}) &= \mathbf{n}_{\partial\Omega_{1(-\infty)}^{(3)}}^T \cdot \mathbf{g}^{(3)}(\mathbf{z}_1^{(3)}, \mathbf{x}_1^{(1)}, t_{m\pm}), \\ G_{\partial\Omega_{1(-\infty)}^{(3)}}^{(1,1)}(\mathbf{z}_1^{(3)}, \mathbf{x}_1^{(1)}, t_{m\pm}) &= \mathbf{n}_{\partial\Omega_{1(-\infty)}^{(3)}}^T \cdot D\mathbf{g}^{(3)}(\mathbf{z}_1^{(3)}, \mathbf{x}_1^{(1)}, t_{m\pm}). \end{aligned} \right\} \quad (22)$$

Using the G-functions, the analytical conditions for stick motion on bottom or top oscillators can be obtained for the passable flow condition from domain $\Omega_1^{(i)}$ to $\Omega_0^{(i)}$ in Luo [29, 30],

$$\left. \begin{aligned} (-1)^\alpha G_{\partial\Omega_{10}^{(\alpha)}}^{(0,1)}(\mathbf{z}_1^{(\alpha)}, \mathbf{x}_1^{(3)}, t_{m-}) < 0, \\ (-1)^\alpha G_{\partial\Omega_{01}^{(\alpha)}}^{(0,0)}(\mathbf{z}_0^{(\alpha)}, \mathbf{x}_0^{(3)}, t_{m+}) < 0. \end{aligned} \right\} \quad (23)$$

$$\left. \begin{aligned} (-1)^\alpha G_{\partial\Omega_{10}^{(3)}}^{(0,1)}(\mathbf{z}_1^{(3)}, \mathbf{x}_1^{(\alpha)}, t_{m-}) > 0, \\ (-1)^\alpha G_{\partial\Omega_{01}^{(3)}}^{(0,0)}(\mathbf{z}_0^{(3)}, \mathbf{x}_0^{(\alpha)}, t_{m+}) > 0. \end{aligned} \right\}$$

Therefore,

$$\left. \begin{aligned} (-1)^\alpha g_1^{(\alpha)}(\mathbf{z}_1^{(\alpha)}, \mathbf{x}_1^{(3)}, t_{m-}) < 0, \\ (-1)^\alpha g_0^{(\alpha)}(\mathbf{z}_0^{(\alpha)}, \mathbf{x}_0^{(3)}, t_{m+}) < 0. \end{aligned} \right\} \quad (24)$$

$$\left. \begin{aligned} (-1)^\alpha g_1^{(3)}(\mathbf{z}_1^{(3)}, \mathbf{x}_1^{(\alpha)}, t_{m-}) > 0, \\ (-1)^\alpha g_0^{(3)}(\mathbf{z}_0^{(3)}, \mathbf{x}_0^{(\alpha)}, t_{m+}) > 0. \end{aligned} \right\}$$

Simplification of the foregoing conditions gives the onset conditions of stick motion on bottom or top oscillators, i.e.,

$$\left. \begin{aligned} \ddot{x}^{(1)}(t_{m\pm}) > \ddot{x}^{(3)}(t_{m\pm}) = -g, \text{ for the bottom,} \\ \ddot{x}^{(2)}(t_{m\pm}) < \ddot{x}^{(3)}(t_{m\pm}) = -g, \text{ for the top,} \end{aligned} \right\} \quad (25)$$

which means that the acceleration of the bottom oscillator $\ddot{x}^{(1)}(t_{m\pm})$ should be larger than the particle's acceleration of $\ddot{x}^{(3)}(t_{m\pm}) = -g$ in order for the particle to stick on the bottom oscillator. However, the acceleration of the top oscillator $\ddot{x}^{(2)}(t_{m\pm})$ should be less than the particle acceleration in order for the particle to stick on the top oscillator. Similarly, the criteria for vanishing of the stick motion from the bottom or top oscillator at $\partial\Omega_{01}^{(\alpha)}$ are from Luo [29, 30],

$$\left. \begin{aligned} G_{\partial\Omega_{01}^{(\alpha)}}^{(0,0)}(\mathbf{z}_0^{(\alpha)}, \mathbf{x}_0^{(3)}, t_{m-}) = 0, \quad (-1)^\alpha G_{\partial\Omega_{01}^{(\alpha)}}^{(0,1)}(\mathbf{z}_0^{(\alpha)}, \mathbf{x}_0^{(3)}, t_{m-}) > 0; \\ G_{\partial\Omega_{01}^{(\alpha)}}^{(1,0)}(\mathbf{z}_1^{(\alpha)}, \mathbf{x}_1^{(3)}, t_{m+}) = 0, \quad (-1)^\alpha G_{\partial\Omega_{01}^{(\alpha)}}^{(1,1)}(\mathbf{z}_1^{(3)}, \mathbf{x}_1^{(\alpha)}, t_{m+}) > 0. \end{aligned} \right\} \quad (26)$$

$$\left. \begin{aligned} G_{\partial\Omega_{01}^{(3)}}^{(0,0)}(\mathbf{z}_0^{(3)}, \mathbf{x}_0^{(\alpha)}, t_{m-}) = 0, \quad (-1)^\alpha G_{\partial\Omega_{01}^{(3)}}^{(0,1)}(\mathbf{z}_0^{(3)}, \mathbf{x}_0^{(\alpha)}, t_{m-}) < 0; \\ G_{\partial\Omega_{01}^{(3)}}^{(1,0)}(\mathbf{z}_1^{(3)}, \mathbf{x}_1^{(\alpha)}, t_{m+}) = 0, \quad (-1)^\alpha G_{\partial\Omega_{01}^{(3)}}^{(1,1)}(\mathbf{z}_1^{(3)}, \mathbf{x}_1^{(\alpha)}, t_{m+}) < 0. \end{aligned} \right\}$$

From the foregoing equations, the relative force relations for $\partial\Omega_{01}^{(\alpha)}$ are

$$\left. \begin{aligned} g_0^{(\alpha)}(\mathbf{z}_0^{(\alpha)}, \mathbf{x}_0^{(3)}, t_{m-}) = 0, (-1)^\alpha \frac{d}{dt} g_0^{(\alpha)}(\mathbf{z}_0^{(\alpha)}, \mathbf{x}_0^{(3)}, t_{m-}) > 0; \\ g_1^{(\alpha)}(\mathbf{z}_1^{(\alpha)}, \mathbf{x}_1^{(3)}, t_{m+}) = 0, (-1)^\alpha \frac{d}{dt} g_1^{(\alpha)}(\mathbf{z}_1^{(\alpha)}, \mathbf{x}_1^{(3)}, t_{m+}) < 0. \\ g_0^{(3)}(\mathbf{z}_0^{(3)}, \mathbf{x}_0^{(\alpha)}, t_{m-}) = 0, (-1)^\alpha \frac{d}{dt} g_0^{(3)}(\mathbf{z}_0^{(3)}, \mathbf{x}_0^{(\alpha)}, t_{m-}) < 0; \\ g_1^{(3)}(\mathbf{z}_1^{(3)}, \mathbf{x}_1^{(\alpha)}, t_{m+}) = 0, (-1)^\alpha \frac{d}{dt} g_1^{(3)}(\mathbf{z}_1^{(3)}, \mathbf{x}_1^{(\alpha)}, t_{m+}) > 0. \end{aligned} \right\} \quad (27)$$

With the relative acceleration and jerk, one gets

$$\left. \begin{aligned} \ddot{x}^{(1)}(t_{m\pm}) = \ddot{x}^{(3)}(t_{m\pm}) = -g, \\ \ddot{x}_{m\pm}^{(1)} < \ddot{x}_{m\pm}^{(3)} = 0, \\ \ddot{x}^{(2)}(t_{m\pm}) = \ddot{x}^{(3)}(t_{m\pm}) = -g, \\ \ddot{x}_{m\pm}^{(2)} > \ddot{x}_{m\pm}^{(3)} = 0, \end{aligned} \right\} \begin{array}{l} \text{for the bottom,} \\ \text{for the top.} \end{array} \quad (28)$$

Using the G-functions of the flow to each boundary, the conditions of grazing motions are from Luo [29, 30], i.e.,

$$\left. \begin{aligned} (-1)^\alpha G_{\partial\Omega_{1(-\infty)}^{(1,0)}}(\mathbf{z}_1^{(\alpha)}, \mathbf{x}_1^{(3)}, t_{m\pm}) = 0, \text{ and } (-1)^\alpha G_{\partial\Omega_{1(-\infty)}^{(1,1)}}(\mathbf{z}_1^{(\alpha)}, \mathbf{x}_1^{(3)}, t_{m\pm}) > 0 \text{ for } \partial\Omega_{1(-\infty)}^{(\alpha)}; \\ (-1)^\alpha G_{\partial\Omega_{1(+\infty)}^{(1,0)}}(\mathbf{z}_1^{(\alpha)}, \mathbf{x}_1^{(3)}, t_{m\pm}) = 0, \text{ and } (-1)^\alpha G_{\partial\Omega_{1(+\infty)}^{(1,1)}}(\mathbf{z}_1^{(\alpha)}, \mathbf{x}_1^{(3)}, t_{m\pm}) > 0 \text{ for } \partial\Omega_{1(+\infty)}^{(\alpha)}; \\ (-1)^\alpha G_{\partial\Omega_{1(-\infty)}^{(3,0)}}(\mathbf{z}_1^{(3)}, \mathbf{x}_1^{(\alpha)}, t_{m\pm}) = 0, \text{ and } (-1)^\alpha G_{\partial\Omega_{1(-\infty)}^{(3,1)}}(\mathbf{z}_1^{(3)}, \mathbf{x}_1^{(\alpha)}, t_{m\pm}) < 0 \text{ for } \partial\Omega_{1(-\infty)}^{(\alpha)}; \\ (-1)^\alpha G_{\partial\Omega_{1(+\infty)}^{(3,0)}}(\mathbf{z}_1^{(3)}, \mathbf{x}_1^{(\alpha)}, t_{m\pm}) = 0, \text{ and } (-1)^\alpha G_{\partial\Omega_{1(+\infty)}^{(3,1)}}(\mathbf{z}_1^{(3)}, \mathbf{x}_1^{(\alpha)}, t_{m\pm}) < 0 \text{ for } \partial\Omega_{1(+\infty)}^{(\alpha)}. \end{aligned} \right\} \quad (29)$$

So the grazing motion conditions on the bottom and top for the non-stick motion boundaries are

$$\left. \begin{aligned} \dot{x}^{(3)} = \dot{x}^{(1)} \text{ and } \ddot{x}^{(1)} < \ddot{x}^{(3)} = -g \text{ for } \partial\Omega_{1(-\infty)}^{(1)}, \partial\Omega_{1(-\infty)}^{(3)}; \\ \dot{x}^{(3)} = \dot{x}^{(2)} \text{ and } \ddot{x}^{(2)} > \ddot{x}^{(3)} = -g \text{ for } \partial\Omega_{1(+\infty)}^{(2)}, \partial\Omega_{1(+\infty)}^{(3)}. \end{aligned} \right\} \quad (30)$$

Similarly, the grazing conditions for stick motion boundaries are from Luo [29, 30], i.e.,

$$\left. \begin{aligned} G_{\partial\Omega_{10}^{(1,0)}}(\mathbf{z}_1^{(\alpha)}, \mathbf{x}_1^{(3)}, t_{m\pm}) = 0, \text{ and } (-1)^\alpha G_{\partial\Omega_{10}^{(1,1)}}(\mathbf{z}_1^{(\alpha)}, \mathbf{x}_1^{(3)}, t_{m\pm}) > 0 \text{ for } \partial\Omega_{10}^{(\alpha)}, \\ G_{\partial\Omega_{01}^{(0,0)}}(\mathbf{z}_0^{(\alpha)}, \mathbf{x}_0^{(3)}, t_{m\pm}) = 0, \text{ and } (-1)^\alpha G_{\partial\Omega_{01}^{(0,1)}}(\mathbf{z}_0^{(\alpha)}, \mathbf{x}_0^{(3)}, t_{m\pm}) < 0 \text{ for } \partial\Omega_{01}^{(\alpha)}. \\ G_{\partial\Omega_{10}^{(3,0)}}(\mathbf{z}_1^{(3)}, \mathbf{x}_1^{(\alpha)}, t_{m\pm}) = 0, \text{ and } (-1)^\alpha G_{\partial\Omega_{10}^{(3,1)}}(\mathbf{z}_1^{(3)}, \mathbf{x}_1^{(\alpha)}, t_{m\pm}) < 0 \text{ for } \partial\Omega_{10}^{(\alpha)}, \\ G_{\partial\Omega_{01}^{(0,0)}}(\mathbf{z}_0^{(3)}, \mathbf{x}_0^{(\alpha)}, t_{m\pm}) = 0, \text{ and } (-1)^\alpha G_{\partial\Omega_{01}^{(0,1)}}(\mathbf{z}_0^{(3)}, \mathbf{x}_0^{(\alpha)}, t_{m\pm}) > 0 \text{ for } \partial\Omega_{01}^{(\alpha)}. \end{aligned} \right\} \quad (31)$$

The corresponding accelerations and jerks should satisfy the following relations.

$$\left. \begin{aligned} \ddot{x}^{(1)} = \ddot{x}^{(3)} = -g \text{ and } \ddot{x}^{(1)} < \ddot{x}^{(3)} = 0 \text{ for } \partial\Omega_{10}^{(1)}, \partial\Omega_{10}^{(3)}, \\ \ddot{x}^{(1)} = \ddot{x}^{(3)} = -g \text{ and } \ddot{x}^{(1)} > \ddot{x}^{(3)} = 0 \text{ for } \partial\Omega_{01}^{(1)}, \partial\Omega_{01}^{(3)}, \\ \ddot{x}^{(2)} = \ddot{x}^{(3)} = -g \text{ and } \ddot{x}^{(2)} > \ddot{x}^{(3)} = 0 \text{ for } \partial\Omega_{10}^{(2)}, \partial\Omega_{10}^{(3)}, \\ \ddot{x}^{(2)} = \ddot{x}^{(3)} = -g \text{ and } \ddot{x}^{(2)} < \ddot{x}^{(3)} = 0 \text{ for } \partial\Omega_{01}^{(2)}, \partial\Omega_{01}^{(3)}, \end{aligned} \right\} \begin{array}{l} \text{for bottom;} \\ \text{for top.} \end{array} \quad (32)$$

Periodic solutions and stability

Using the discontinuous boundaries in Eq.(6), the switching sets of the Fermi oscillator without stick are introduced as

$$\left. \begin{aligned} \Sigma_{1(-\infty)} &= \Sigma_{1(-\infty)}^{(1)} \otimes \Sigma_{1(-\infty)}^{(2)} \otimes \Sigma_{1(-\infty)}^{(3)} \\ &= \left\{ (x_k^{(1)}, \dot{x}_k^{(1)}, x_k^{(2)}, \dot{x}_k^{(2)}, x_k^{(3)}, \dot{x}_k^{(3)}, t_k) \mid x_k^{(3)} = x_{k+}^{(1)}, \dot{x}_k^{(3)} \neq \dot{x}_k^{(1)} \right\}, \\ \Sigma_{1(+\infty)} &= \Sigma_{1(+\infty)}^{(1)} \otimes \Sigma_{1(+\infty)}^{(2)} \otimes \Sigma_{1(+\infty)}^{(3)} \\ &= \left\{ (x_k^{(1)}, \dot{x}_k^{(1)}, x_k^{(2)}, \dot{x}_k^{(2)}, x_k^{(3)}, \dot{x}_k^{(3)}, t_k) \mid x_k^{(3)} = x_{k+}^{(2)}, \dot{x}_k^{(3)} \neq \dot{x}_k^{(2)} \right\}, \end{aligned} \right\} \quad (33)$$

where the switching sets $\Sigma_{1(-\infty)}^{(i)}$ and $\Sigma_{1(+\infty)}^{(i)}$ are defined on boundary $\partial\Omega_{1(-\infty)}^{(i)}$ and $\partial\Omega_{1(+\infty)}^{(i)}$, respectively. The corresponding definitions for the top and bottom oscillators plus the particle are given as

$$\left. \begin{aligned} \Sigma_{1(-\infty)}^{(i)} &= \left\{ (x_k^{(i)}, \dot{x}_k^{(i)}, t_k) \mid x_k^{(\alpha)} = x_k^{(\bar{\alpha})}, \dot{x}_k^{(\alpha)} \neq \dot{x}_k^{(\bar{\alpha})} \right\} \subset \partial\Omega_{1(-\infty)}^{(i)}, \alpha = 1, 3, \\ \Sigma_{1(+\infty)}^{(i)} &= \left\{ (x_k^{(i)}, \dot{x}_k^{(i)}, t_k) \mid x_k^{(\alpha)} = x_k^{(\bar{\alpha})}, \dot{x}_k^{(\alpha)} \neq \dot{x}_k^{(\bar{\alpha})} \right\} \subset \partial\Omega_{1(+\infty)}^{(i)}, \alpha = 2, 3. \end{aligned} \right\} \quad (34)$$

Thus, the generic mappings for motions without stick motion are

$$\begin{aligned} P_1 : \Sigma_{1(-\infty)} &\rightarrow \Sigma_{1(+\infty)}, P_2 : \Sigma_{1(+\infty)} \rightarrow \Sigma_{1(-\infty)}, \\ P_3 : \Sigma_{1(-\infty)} &\rightarrow \Sigma_{1(-\infty)}, P_4 : \Sigma_{1(+\infty)} \rightarrow \Sigma_{1(+\infty)}. \end{aligned} \quad (35)$$

From the above definitions, the switching subsets and the sub-mappings without stick motion are sketched in Figure 6 (a) and (b) for the bottom and top oscillators, respectively. In Figure 6 (c), the sub-mappings without stick motion for the particle are presented.

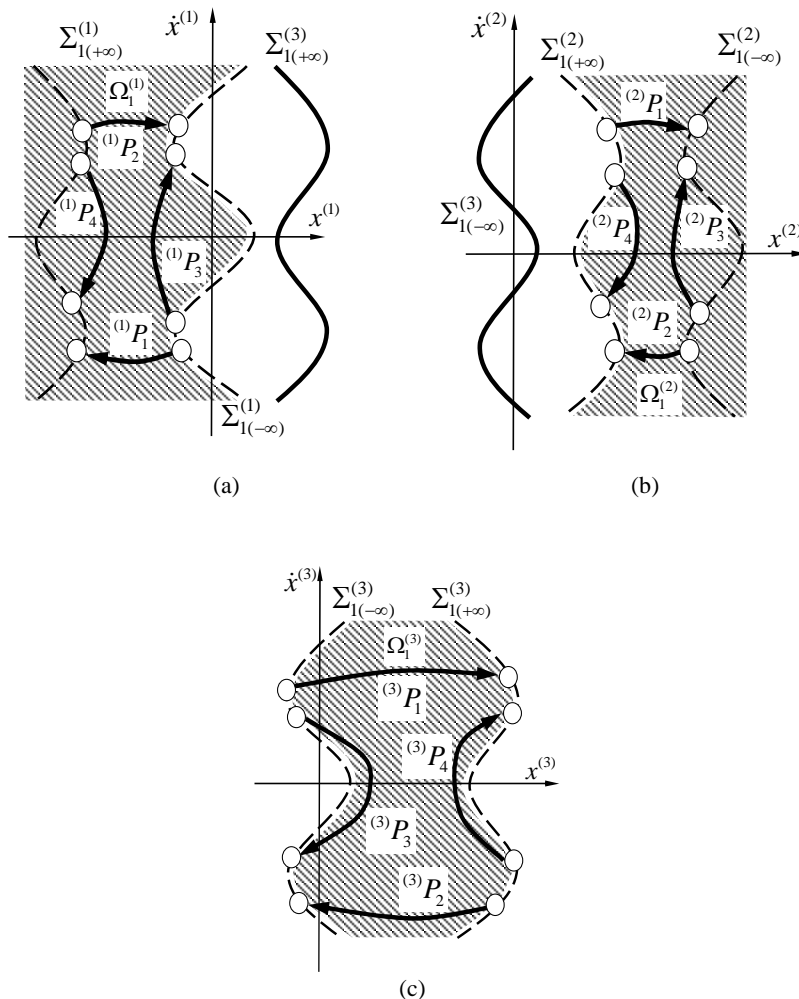
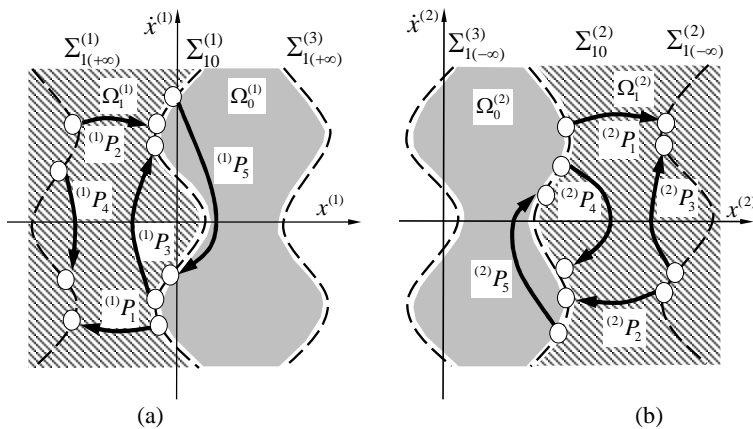


Fig. 6. Switching sets and generic mappings for non-stick motion in absolute coordinates: (a) bottom oscillator, (b) top oscillator, and (c) particle



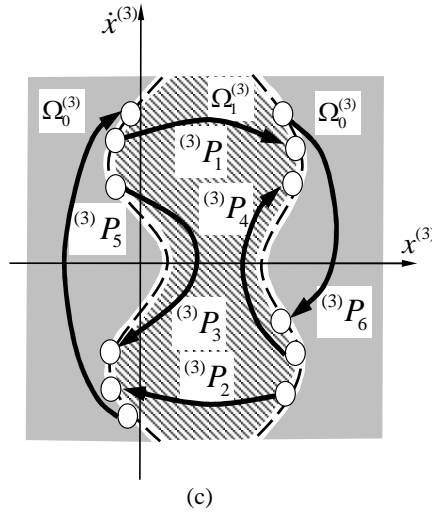


Fig. 7. Switching sets and generic mappings for stick motion in absolute coordinates: (a) bottom oscillator, (b) top oscillator, and (c) particle

They are given by:

$$\begin{aligned}
 P_1 &= ({}^{(1)}P_1, {}^{(2)}P_1, {}^{(3)}P_1), P_2 = ({}^{(1)}P_2, {}^{(2)}P_2, {}^{(3)}P_2), \\
 P_3 &= ({}^{(1)}P_3, {}^{(2)}P_3, {}^{(3)}P_3), P_4 = ({}^{(1)}P_4, {}^{(2)}P_4, {}^{(3)}P_4),
 \end{aligned} \tag{36}$$

$$\begin{aligned}
 {}^{(i)}P_1 : \Sigma_{1(-\infty)}^{(i)} &\rightarrow \Sigma_{1(+\infty)}^{(i)}, \quad {}^{(i)}P_2 : \Sigma_{1(+\infty)}^{(i)} \rightarrow \Sigma_{1(-\infty)}^{(i)}, \\
 {}^{(i)}P_3 : \Sigma_{1(-\infty)}^{(i)} &\rightarrow \Sigma_{1(-\infty)}^{(i)}, \quad {}^{(i)}P_4 : \Sigma_{1(+\infty)}^{(i)} \rightarrow \Sigma_{1(+\infty)}^{(i)}.
 \end{aligned} \tag{37}$$

Similarly, the switching subsets and the sub-mappings with stick motion are presented in Figure 7 (a) and (b) for the bottom and top oscillators, respectively. The sub-mappings with stick motion for the particle are sketched in Figure 7 (c). From the boundaries in Eq. (6) and (8), the switching sets of the Fermi oscillator with stick motion are defined as

$$\left. \begin{aligned}
 {}_\alpha \Sigma_{10} &= {}_\alpha \Sigma_{10}^{(1)} \otimes {}_\alpha \Sigma_{10}^{(2)} \otimes {}_\alpha \Sigma_{10}^{(3)} \\
 &= \left\{ (x_k^{(\bar{\alpha})}, \dot{x}_k^{(\bar{\alpha})}, x_k^{(\alpha)}, \dot{x}_k^{(\alpha)}, x_k^{(3)}, \dot{x}_k^{(3)}, t_k) \mid x_k^{(3)} = x_k^{(\alpha)}, \dot{x}_k^{(3)} = \dot{x}_k^{(\alpha)} \right\}, \\
 \Sigma_{1(-\infty)} &= \Sigma_{1(-\infty)}^{(1)} \otimes \Sigma_{1(-\infty)}^{(2)} \otimes \Sigma_{1(-\infty)}^{(3)} \\
 &= \left\{ (x_k^{(1)}, \dot{x}_k^{(1)}, x_k^{(2)}, \dot{x}_k^{(2)}, x_k^{(3)}, \dot{x}_k^{(3)}, t_k) \mid x_k^{(3)} = x_k^{(1)}, \dot{x}_k^{(3)} \neq \dot{x}_k^{(1)} \right\}, \\
 \Sigma_{1(+\infty)} &= \Sigma_{1(+\infty)}^{(1)} \otimes \Sigma_{1(+\infty)}^{(2)} \otimes \Sigma_{1(+\infty)}^{(3)} \\
 &= \left\{ (x_k^{(1)}, \dot{x}_k^{(1)}, x_k^{(2)}, \dot{x}_k^{(2)}, x_k^{(3)}, \dot{x}_k^{(3)}, t_k) \mid x_k^{(3)} = x_k^{(2)}, \dot{x}_k^{(3)} \neq \dot{x}_k^{(2)} \right\},
 \end{aligned} \right\} \tag{38}$$

where $\alpha = 1, 2$ with $\bar{\alpha} = 2, 1$. The switching set ${}_{\alpha}\Sigma_{10}$ is defined on the boundary $\partial\Omega_{10}$:

$$\begin{aligned} {}_{\alpha}\Sigma_{10}^{(i)} &= \left\{ (x_k^{(i)}, \dot{x}_k^{(i)}, t_k) \left| \begin{array}{l} x_k^{(3)} = x_k^{(\alpha)}, \\ \dot{x}_k^{(3)} = \dot{x}_k^{(\alpha)}, \end{array} \right. \right\} \subset \partial\Omega_{10}^{(i)}, \text{ for } \alpha = 1, 2; i = 1, 2, 3; \\ \Sigma_{1(-\infty)}^{(i)} &= \left\{ (x_k^{(i)}, \dot{x}_k^{(i)}, t_i) \left| \begin{array}{l} x_k^{(3)} = x_k^{(1)}, \\ \dot{x}_k^{(3)} \neq \dot{x}_k^{(1)}, \end{array} \right. \right\} \subset \partial\Omega_{1(-\infty)}^{(i)}, \text{ for } i = 1, 3; \\ \Sigma_{1(+\infty)}^{(i)} &= \left\{ (x_k^{(i)}, \dot{x}_k^{(i)}, t_i) \left| \begin{array}{l} x_k^{(3)} = x_k^{(2)}, \\ \dot{x}_k^{(3)} \neq \dot{x}_k^{(2)}, \end{array} \right. \right\} \subset \partial\Omega_{1(+\infty)}^{(i)}, \text{ for } i = 2, 3. \end{aligned} \quad (39)$$

Thus, the generic mappings for the stick motion are defined as

$$\begin{aligned} P_1 : \Sigma_{10}^{(1)} &\rightarrow \Sigma_{1(+\infty)}, \text{ or } \Sigma_{1(-\infty)} \rightarrow \Sigma_{10}^{(2)}, \\ P_2 : \Sigma_{1(+\infty)} &\rightarrow \Sigma_{10}^{(1)}, \text{ or } \Sigma_{10}^{(2)} \rightarrow \Sigma_{1(-\infty)}, \\ P_3 : \Sigma_{1(-\infty)} &\rightarrow \Sigma_{10}^{(1)}, P_4 : \Sigma_{10}^{(2)} \rightarrow \Sigma_{1(+\infty)}, \\ P_5 : \Sigma_{10}^{(1)} &\rightarrow \Sigma_{10}^{(1)}, \text{ and } P_6 : \Sigma_{10}^{(2)} \rightarrow \Sigma_{10}^{(2)}. \end{aligned} \quad (40)$$

where the global mappings of P_1 and P_2 will map from one switching set to another. The local mappings of ($P_3, P_4, P_5,$ and P_6) map from one switching set to itself, as in Figs. 6 and 7. From the above definitions, the governing equations for generic mapping P_j ($j=1, 2, 3, 4$) can be expressed by

$$\mathbf{f}^{(j)}(\mathbf{Y}_k, \mathbf{Y}_{k+1}) = \mathbf{0} \text{ for } P_j, \quad (41)$$

with

$$\begin{aligned} \mathbf{f}^{(j)} &= (f_1^{(j)}, f_2^{(j)}, f_3^{(j)}, f_4^{(j)}, f_5^{(j)}, f_6^{(j)})^T, \\ \mathbf{Y}_k &= (x_k^{(1)}, \dot{x}_k^{(1)}, x_k^{(2)}, \dot{x}_k^{(2)}, x_k^{(3)}, \dot{x}_k^{(3)}, t_k)^T, \\ \mathbf{Y}_{k+1} &= (x_{k+1}^{(1)}, \dot{x}_{k+1}^{(1)}, x_{k+1}^{(2)}, \dot{x}_{k+1}^{(2)}, x_{k+1}^{(3)}, \dot{x}_{k+1}^{(3)}, t_{k+1})^T; \\ &\left. \begin{array}{l} x_k^{(3)} = x_k^{(1)} \text{ and } x_{k+1}^{(3)} = x_{k+1}^{(2)} \text{ for } P_1, \\ x_k^{(3)} = x_k^{(2)} \text{ and } x_{k+1}^{(3)} = x_{k+1}^{(1)} \text{ for } P_2, \\ x_k^{(3)} = x_k^{(1)} \text{ and } x_{k+1}^{(3)} = x_{k+1}^{(1)} \text{ for } P_3, \\ x_k^{(3)} = x_k^{(2)} \text{ and } x_{k+1}^{(3)} = x_{k+1}^{(2)} \text{ for } P_4. \end{array} \right\} \quad (42) \end{aligned}$$

The governing equations for the stick mapping $P_5^{(\alpha)}$ and $P_6^{(\alpha)}$ can be expressed as

$$\mathbf{f}^{(j)}(\mathbf{Z}_k^{(j)}, \mathbf{Z}_{k+1}^{(j)}) = 0 \text{ for } P_j^{(\alpha)} \quad (j = 5, 6), \quad (43)$$

and

$$\begin{aligned} \mathbf{Z}_k^{(j)} &= (x_k^{(\bar{\alpha})}, \dot{x}_k^{(\bar{\alpha})}, x_k^{(3)}, \dot{x}_k^{(3)}, t_k)^T, \\ \mathbf{Z}_{k+1}^{(j)} &= (x_{k+1}^{(\bar{\alpha})}, \dot{x}_{k+1}^{(\bar{\alpha})}, x_{k+1}^{(3)}, \dot{x}_{k+1}^{(3)}, t_{k+1})^T, \\ \mathbf{f}^{(j)} &= (\bar{\alpha})f_1^{(0)}, (\bar{\alpha})f_2^{(0)}, (3)f_1^{(0)}, (3)f_2^{(0)}, (\alpha)f_5^{(0)} \Big)^T, \\ (\alpha)f_5^{(0)} &= g_1^{(\alpha)}(0, \mathbf{x}_{k+1}^{(\alpha)}, t_{k+1}). \\ \left. \begin{aligned} x_k^{(3)} &= x_k^{(\alpha)} \text{ and } \dot{x}_k^{(3)} = \dot{x}_k^{(\alpha)}, x_{k+1}^{(3)} = x_{k+1}^{(\alpha)} \text{ and } \dot{x}_{k+1}^{(3)} = \dot{x}_{k+1}^{(\alpha)}, \\ (-1)^\alpha \ddot{x}_k^{(\alpha)} &< (-1)^{\alpha+1} g, \text{ and } (-1)^\alpha \ddot{x}_{k+1}^{(\alpha)} > (-1)^{\alpha+1} g, \end{aligned} \right\} \\ &\text{with } j = 5, 6 \text{ for } (\alpha, \bar{\alpha}) = (1, 2) \text{ and } (2, 1). \end{aligned} \quad (44)$$

The notation for mapping action is introduced as

$$P_{j_k j_{k-1} \dots j_1} = P_{j_k} \circ P_{j_{k-1}} \circ \dots \circ P_{j_1}, \quad (45)$$

where $j_k \in \{1, 2, 3, 4, 5, 6\}$ is a positive integer. For a motion with m -time repeated mapping structure of $P_{j_1 j_2 \dots j_k}$, the total mapping structure can be expressed as

$$P_{j_k j_{k-1} \dots j_1}^{(m)} = \underbrace{(P_{j_k} \circ P_{j_{k-1}} \circ \dots \circ P_{j_1}) \circ \dots \circ (P_{j_k} \circ P_{j_{k-1}} \circ \dots \circ P_{j_1})}_m = P_{(j_k j_{k-1} \dots j_1)^m}. \quad (46)$$

Consider a motion with a generalized map,

$$P = \underbrace{P_{4^{m_1} 0^{k_{31}} 2^{k_{21}} 3^{n_1} 1^{k_{11}}} \circ \dots \circ P_{4^{m_l} 0^{k_{31}} 2^{k_{21}} 3^{n_l} 1^{k_{11}}}}_{l\text{-terms}} = P_{\underbrace{(4^{m_1} 0^{k_{31}} 2^{k_{21}} 3^{n_1} 1^{k_{11}}) \dots (4^{m_l} 0^{k_{31}} 2^{k_{21}} 3^{n_l} 1^{k_{11}})}}_{l\text{-terms}}}, \quad (47)$$

where $k_{js} \in \{0, 1\}$ and $m_s, n_s \in \mathbb{N}$ ($s = 1, 2, \dots, l$). Define vectors $\mathbf{X}_k \equiv (X_{k1}, X_{k2}, X_{k3}, X_{k4}, X_{k5}, X_{k6})^T$ ($X_{kr} \in \{x_k^{(1)}, \dot{x}_k^{(1)}, x_k^{(2)}, \dot{x}_k^{(2)}, x_k^{(3)}, \dot{x}_k^{(3)}, t_k\}$) and $\mathbf{Y}_k \equiv (Y_{k1}, Y_{k2}, Y_{k3}, Y_{k4}, Y_{k5}, Y_{k6})^T$ ($Y_{kr} \in \{x_k^{(1)}, \dot{x}_k^{(1)}, x_k^{(2)}, \dot{x}_k^{(2)}, x_k^{(3)}, \dot{x}_k^{(3)}, t_k\}$). The motion pertaining to the mapping structure in Eq. (47) can be determined by

$$\mathbf{Y}_{k+\sum_{s=1}^l (m_s+k_{3s}+k_{2s}+n_s+k_{1s})} = P \mathbf{X}_k = P_{\underbrace{(4^{m_1} 0^{k_{31}} 2^{k_{21}} 3^{n_1} 1^{k_{11}}) \dots (4^{m_l} 0^{k_{31}} 2^{k_{21}} 3^{n_l} 1^{k_{11}})}}_{l\text{-terms}}} \mathbf{X}_k. \quad (48)$$

From the algebraic equations for generic mappings in Eqs. (41)-(44), one can obtain a set of nonlinear algebraic equations for such a mapping structure, i.e.,

$$\left. \begin{aligned} \mathbf{f}^{(1)}(\mathbf{X}_k, \mathbf{Y}_{k+1}) = 0, \dots, \mathbf{f}^{(3)}(\mathbf{X}_{k+k_{1l}}, \mathbf{Y}_{k+k_{1l}+1}) = 0, \dots, \\ \mathbf{f}^{(2)}(\mathbf{X}_{k+k_{1l}+n_l}, \mathbf{Y}_{k+k_{1l}+n_l+1}) = 0, \dots, \\ \mathbf{f}^{(4)}(\mathbf{X}_{k+\sum_{s=1}^l(m_s+k_{3s}+k_{2s}+n_s+k_{1s})-1}, \mathbf{Y}_{k+\sum_{s=1}^l(m_s+k_{3s}+k_{2s}+n_s+k_{1s})}) = 0, \\ \mathbf{Y}_{k+\sigma} = \mathbf{X}_{k+\sigma}, \end{aligned} \right\} \quad (49)$$

where $\sigma = 1, \dots, \sum_{s=1}^l(m_s + k_{3s} + k_{2s} + n_s + k_{1s}) - 1$. The periodic motion pertaining to such a mapping requires

$$\mathbf{Y}_{k+\sum_{s=1}^l(n_s+k_{3s}+m_s+k_{2s}+k_{1s})} = \mathbf{X}_k \quad (50)$$

or

$$\left. \begin{aligned} \mathbf{x}_{k+\sum_{s=1}^l(m_s+k_{3s}+k_{2s}+n_s+k_{1s})}^{(i)} &= \mathbf{x}_k^{(i)} \\ \dot{\mathbf{x}}_{k+\sum_{s=1}^l(m_s+k_{3s}+k_{2s}+n_s+k_{1s})}^{(i)} &= \dot{\mathbf{x}}_k^{(i)} \end{aligned} \right\} \text{ for } i = 1, 2, 3 \quad (51)$$

$$\Omega t_{k+\sum_{s=1}^l(m_s+k_{3s}+k_{2s}+n_s+k_{1s})}^{(i)} = \Omega t_k^{(i)} + 2N\pi.$$

Solving Eqs. (49)-(51) generates the switching sets of periodic motion relative to the mapping structure in Eq.(47). Once the switching points for a specific periodic motion are obtained, its local stability and bifurcation analysis can be completed through the corresponding Jacobian matrix. For instance, the Jacobian matrix of the mapping structure in Eq.(48) is computed, i.e.,

$$\begin{aligned} DP &= DP_{\underbrace{(4^{m_l} 0^{k_{3l}} 2^{k_{2l}} 3^{n_l} 1^{k_{1l}}) \dots (4^{m_1} 0^{k_{31}} 2^{k_{21}} 3^{n_1} 1^{k_{11}})}_{l\text{-terms}}} \\ &= \prod_{s=1}^l DP_4^{(m_s)} \cdot DP_0^{(k_{3s})} \cdot DP_2^{(k_{2s})} \cdot DP_3^{(m_s)} \cdot DP_1^{(k_{1s})}, \end{aligned} \quad (52)$$

where

$$DP_\sigma = \left[\frac{\partial \mathbf{Y}_{\sigma+1}}{\partial \mathbf{X}_\sigma} \right]_{6 \times 6} = \left[\frac{\partial Y_{(\sigma+1)i}}{\partial X_{\sigma j}} \right]_{6 \times 6}, \quad (53)$$

for $\sigma = k, k+1, \dots, k + \sum_{s=1}^l(m_s + k_{3s} + k_{2s} + n_s + k_{1s}) - 1$ and all the Jacobian matrix components can be computed through Eq. (49). The variational equation for a set of switching points $\{\mathbf{X}_k^*, \mathbf{Y}_{k+1}^*, \dots, \mathbf{X}_{k+\sum_{s=1}^l(m_s+k_{3s}+k_{2s}+n_s+k_{1s})}^*\}$ is

$$\Delta \mathbf{Y}_{k+\sum_{s=1}^l (m_s+k_{3_s}+k_{2_s}+n_s+k_{1_s})} = DP(\mathbf{X}_k^*) \Delta \mathbf{X}_k. \quad (54)$$

If $\Delta \mathbf{Y}_{k+\sum_{s=1}^l (m_s+k_{3_s}+k_{2_s}+n_s+k_{1_s})} \equiv \lambda \Delta \mathbf{X}_k$, the eigenvalues are computed by

$$\left| DP(\mathbf{X}_k^*) - \lambda \mathbf{I} \right| = 0. \quad (55)$$

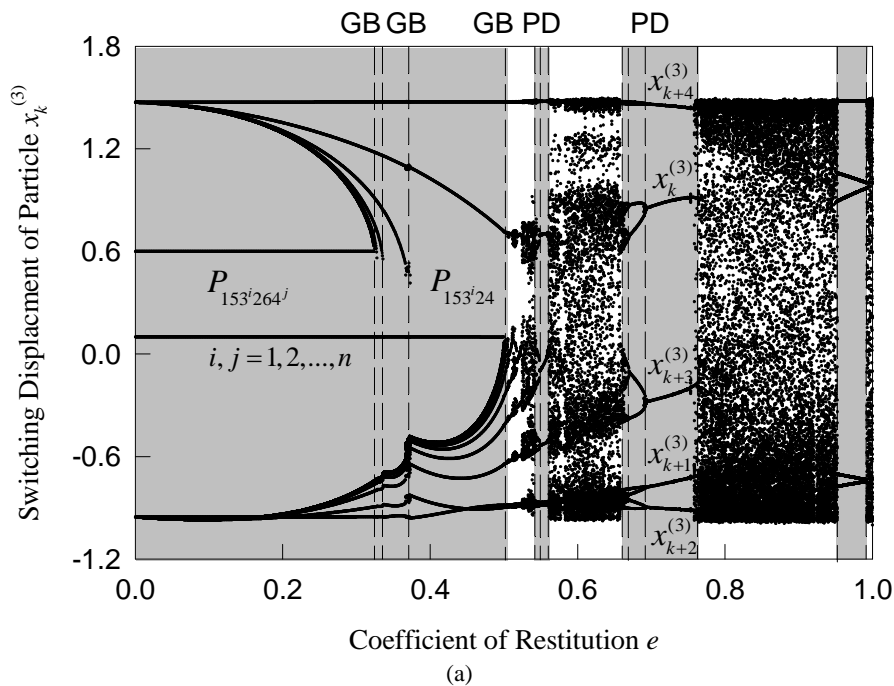
If all $|\lambda_i| < 1$ for $(i=1,2,\dots,6)$, the periodic motion is stable. If one of $|\lambda_i| > 1$ for $(i \in \{1,2,\dots,6\})$, the periodic motion is unstable. If one of $\lambda_i = -1$ and $|\lambda_j| < 1$ for $(i, j \in \{1,2,3,4,5,6\}$ and $j \neq i)$, the period-doubling bifurcation of periodic motion occurs. If one of $\lambda_i = 1$ and $|\lambda_j| < 1$ for $(i, j \in \{1,2,3,4,5,6\}$ and $j \neq i)$, the saddle-node bifurcation of the periodic motion occurs. If $|\lambda_{1,2,3,4}| < 1$ with the complex eigenvalues of $|\lambda_{5,6}| = 1$, the Neimark bifurcation of the periodic motion occurs. However, the eigenvalue analysis cannot be used to predict sticking and grazing motions. Both of them should be determined through the normal vector fields, and the stick motion is determined by Eq. (23) and the grazing bifurcation is determined by Eq. (29) or (31).

Numerical illustrations

Setting $e^{(1)} = e^{(2)} = e$, the bifurcation scenario of varying e for the Fermi oscillator is presented in Figure 8. The parameters are $Q^{(1)} = Q^{(2)} = 20.0$, $\Omega^{(1)} = \Omega^{(2)} = 10.0$, $m^{(1)} = m^{(2)} = 1.0$, $m^{(3)} = 0.01$, $h = 0.5$, $k^{(1)} = k^{(2)} = 80.0$, $c^{(1)} = c^{(2)} = 0.1$. The switching displacement, velocity, and phase of the particle versus the restitution coefficient e are shown in Figure 8 (a)-(c), respectively. The acronyms ‘PD’ and ‘GB’ indicate the period-doubling bifurcation and grazing bifurcation respectively. The shaded areas are for regions of periodic motion. For $e \in (0, 0.5)$, the impact chatter with stick motion exists. In other words, the particle is undergoing the periodic motion where stick motion with top or bottom oscillator occurs after impact chattering. At $e = 0.323, 0.336, 0.371$, and 0.5 , grazing bifurcations occur and the current periodic motion disappears, and another different periodic motion starts.

With the same parameters the analytical prediction of periodic motions with varying the restitution coefficient e is presented in Figure 9. The displacement, velocity, and switching phase of the particle versus the coefficient of restitution e are shown in Figure 9 (a), (b), and (c), respectively. The solid and dotted curves represent the stable and unstable solutions, respectively. The acronyms ‘PD’, ‘SN’, ‘NB’, and ‘GB’ represent the period doubling bifurcation, saddle node bifurcation, Neimark bifurcation, and grazing bifurcation, respectively. For $e \in (0, 0.5)$, the periodic motion of impact chatter with stick exists. At $e = 0.323, 0.336, 0.371$, and 0.5 , the grazing bifurcations occur. For $e \in (0.5396, 0.5522)$, the stable periodic motion of $P_{(3^3 241)^2}$ exists. At $e = 0.5396$, a period doubling bifurcation occurs. At $e = 0.5522$, a saddle-node bifurcation of periodic motion of $P_{(3^3 241)^2}$ occurs and this periodic motion disappears. Such a value of $e = 0.5522$ is also for period-doubling of periodic motion of $P_{3^3 241}$. The stable periodic motion of $P_{3^3 241}$ exists in the region of

$e \in (0.5522, 0.5626)$. At $e = 0.5626$, the saddle-node bifurcation of periodic motion of $P_{3^3 241}$ occurs, and such a periodic motion disappears. For $e \in (0.6688, 0.6960)$, the stable periodic motion of $P_{(413^2 2)^2}$ exists. At $e = 0.6688$, a period doubling bifurcation occurs, and the periodic motion of $P_{(413^2 2)^2}$ becomes unstable. At $e = 0.6960$, a saddle node bifurcation of periodic motion of $P_{(413^2 2)^2}$ takes place, and the periodic motion of $P_{(413^2 2)^2}$ vanishes. However, the periodic motion of $P_{413^2 2}$ starts; this corresponds to the period doubling bifurcation of $P_{413^2 2}$ motion, where the motion becomes unstable. The stable periodic motion of $P_{413^2 2}$ lies in $e \in (0.6960, 0.7668)$. At $e = 0.7668$ the stable periodic motion of $P_{413^2 2}$ disappears because of the saddle-node bifurcation. Finally, for $e \in (0.9042, 1.0)$, the stable periodic motion of P_{1324^2} is observed. At $e = 0.9042$ and 1, the Neimark bifurcation of the periodic motion of P_{1324^2} takes place. The prediction stops at $e = 1.0$ because the restitution coefficient cannot be greater than one. The real parts, imaginary parts, and magnitudes of the eigenvalues are illustrated in Figure 9 (d)-(f), respectively.



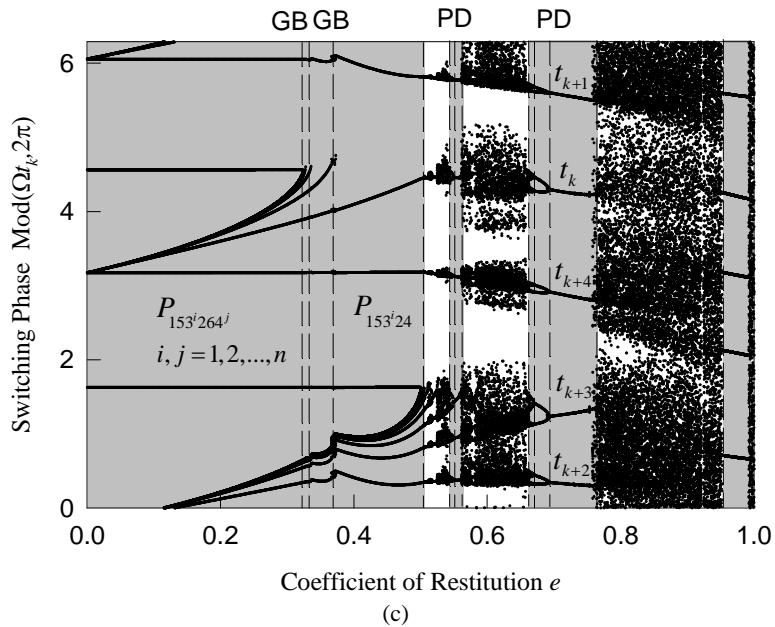
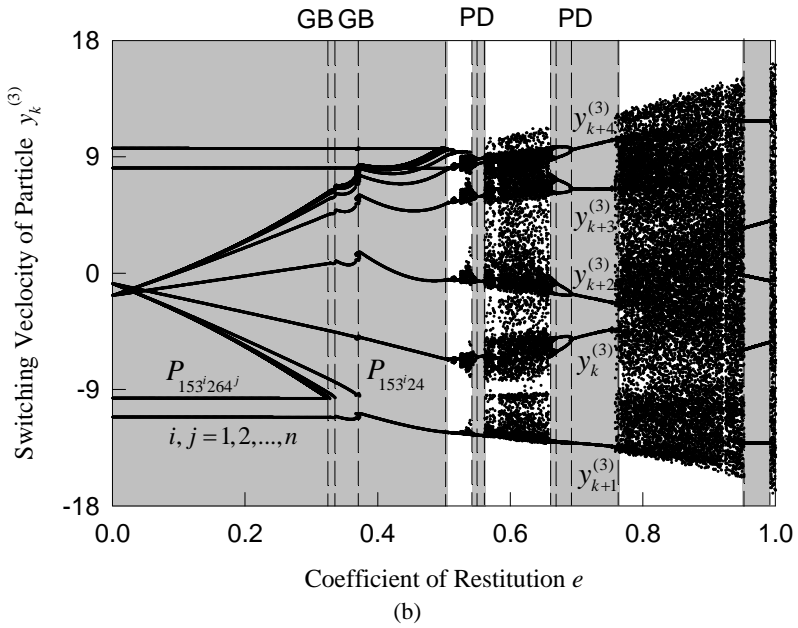
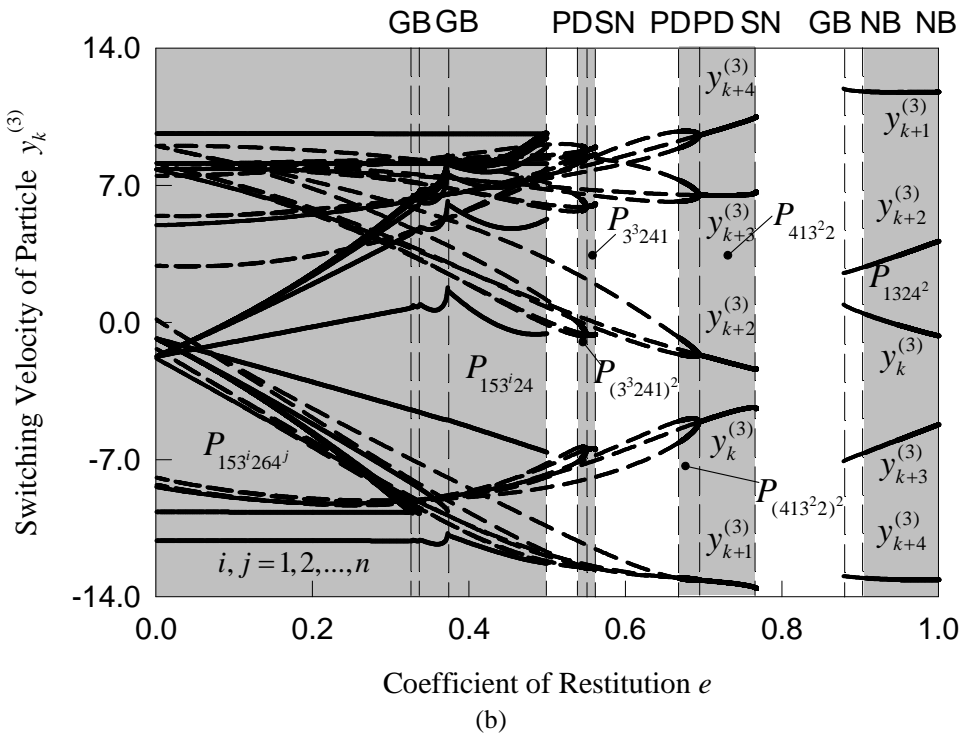
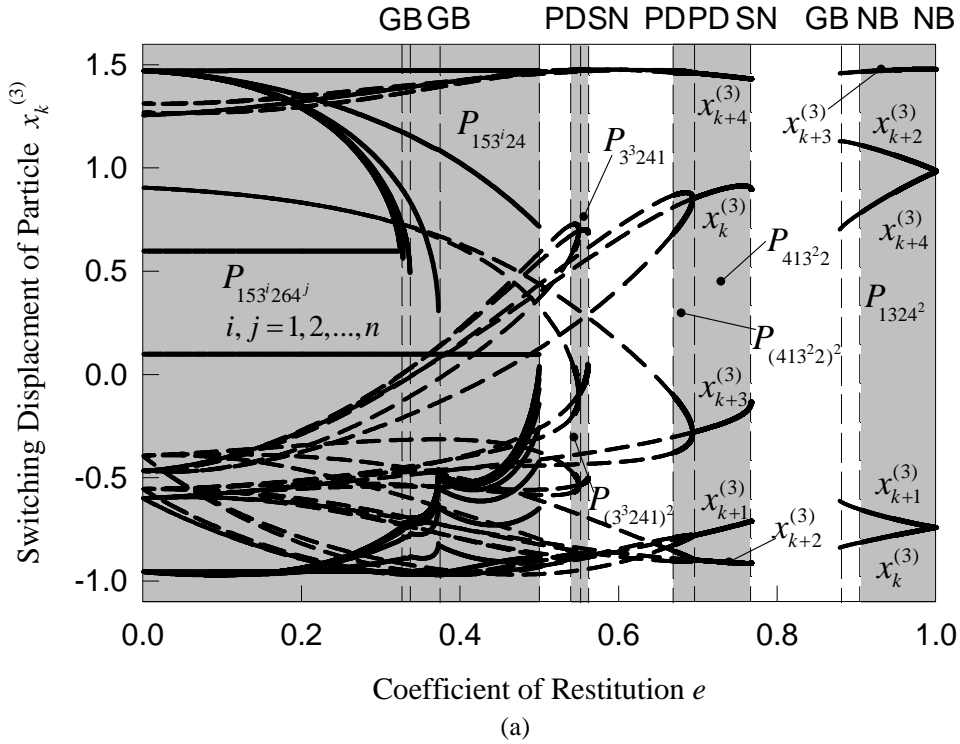
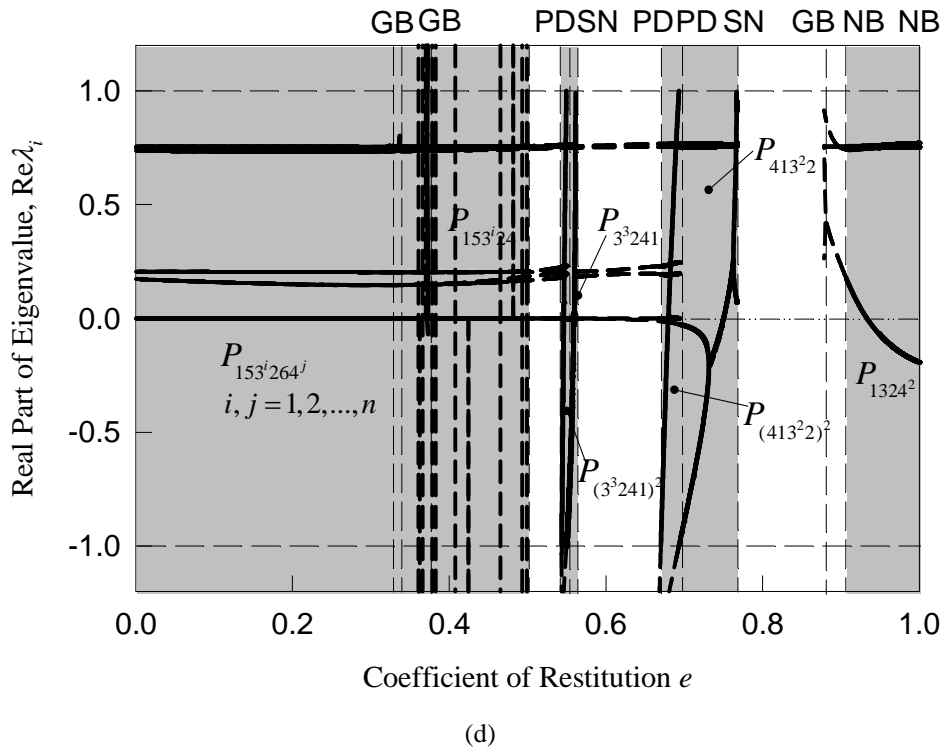
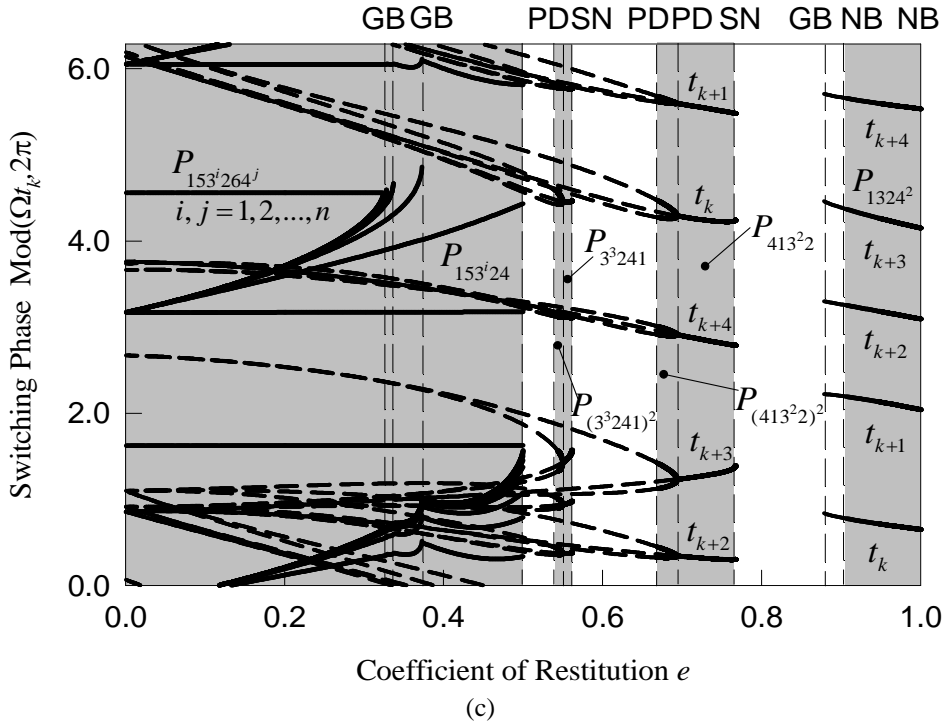


Fig. 8. Bifurcation scenario of varying restitution coefficient e : (a) displacement of particle, (b) velocity of particle, and (c) switching phase. ($Q^{(1)} = Q^{(2)} = 20.0$, $\Omega^{(1)} = \Omega^{(2)} = 10.0$, $m^{(1)} = m^{(2)} = 1.0$, $m^{(3)} = 0.01$, $h = 0.5$, $k^{(1)} = k^{(2)} = 80.0$, $c^{(1)} = c^{(2)} = 0.1$)





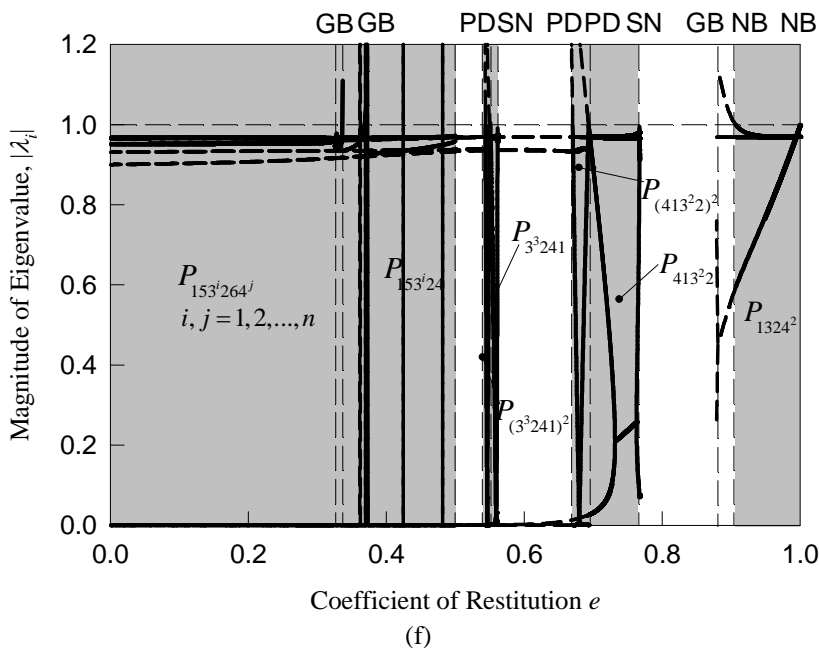
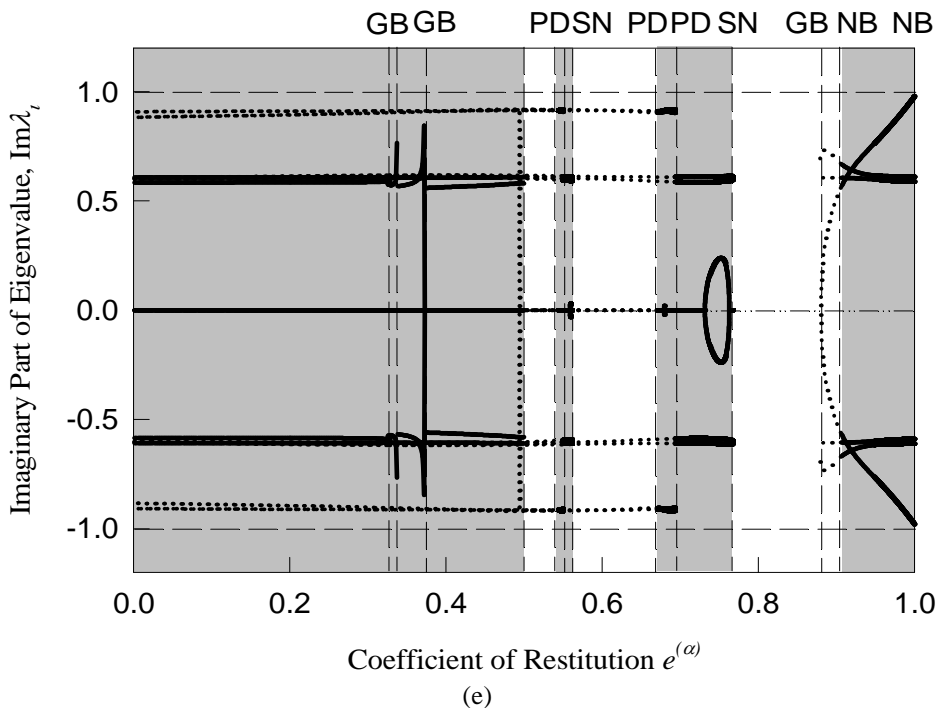
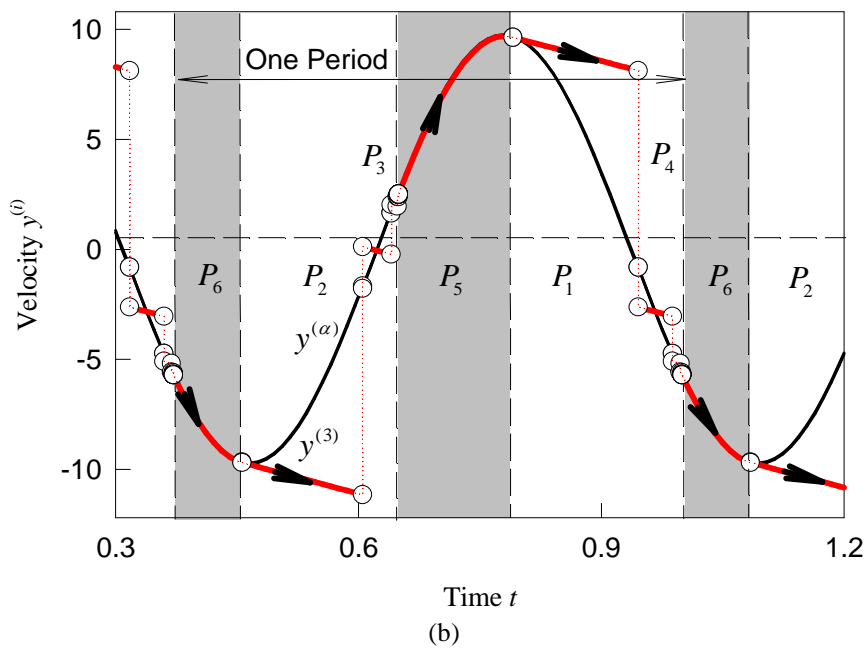
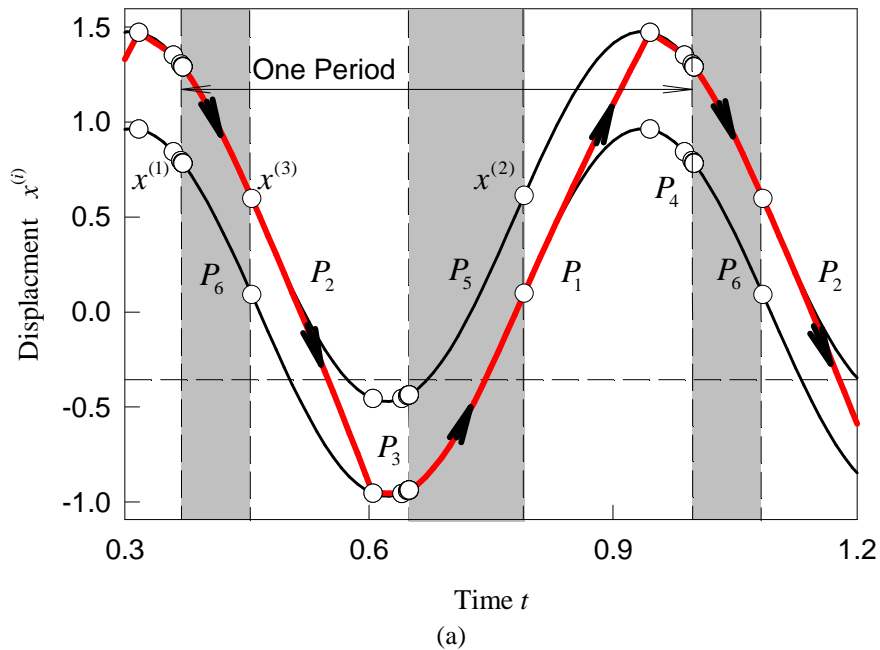
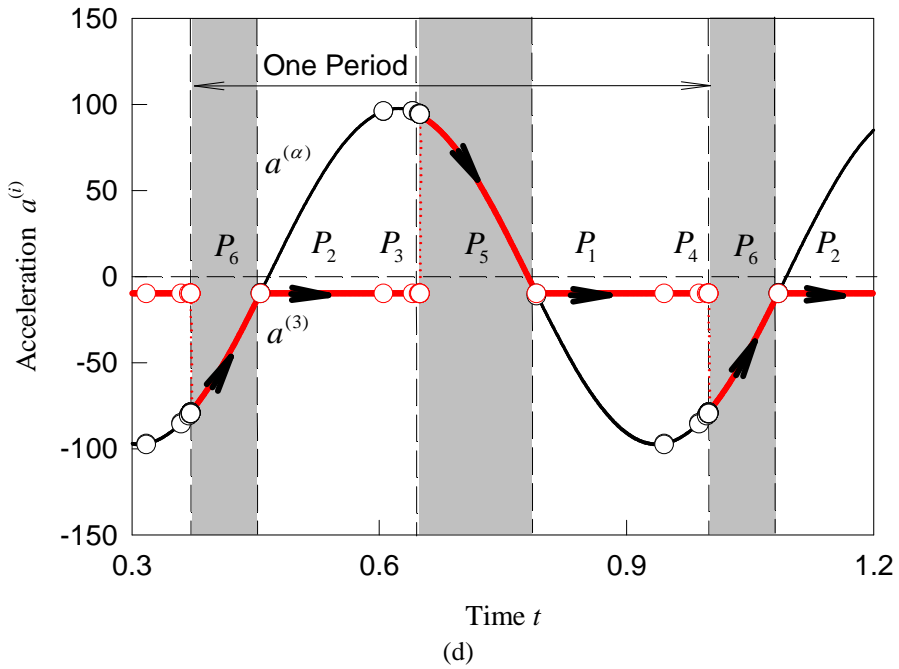
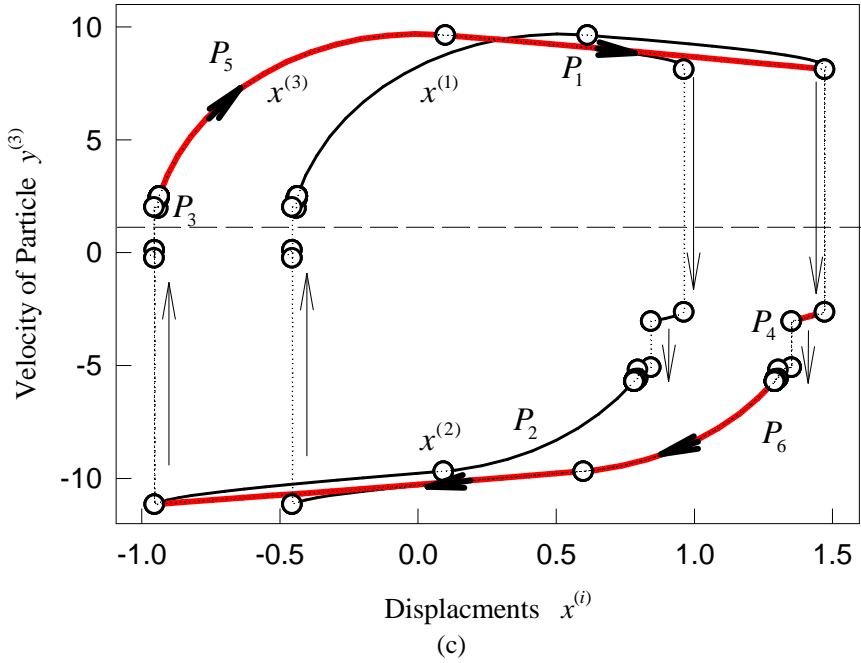


Fig. 9. Analytical prediction of varying the restitution coefficient of impact e : (a) switching displacement of particle, (b) switching velocity of particle, (c) switching phase, (d) real part of eigenvalues, (e) imaginary part of eigenvalues, and (f) magnitude of eigenvalues. ($Q^{(1)} = Q^{(2)} = 20.0$, $\Omega^{(1)} = \Omega^{(2)} = 10.0$, $m^{(1)} = m^{(2)} = 1.0$, $m^{(3)} = 0.01$, $h = 0.5$, $k^{(1)} = k^{(2)} = 80.0$, $c^{(1)} = c^{(2)} = 0.1$)

Using the same parameters, a periodic motion of $P_{153^7 264^7}$ is illustrated with $e = 0.2$ in Figure 10. The initial conditions are $x_0^{(1)} = 0.79534917$, $\dot{x}_0^{(1)} = -5.49025226$, $x_0^{(2)} = 1.30373854$, $\dot{x}_0^{(2)} = -5.51085936$, $x_0^{(3)} = 1.30373854$, $\dot{x}_0^{(3)} = -5.57828916$ for $t_0 = 0.368919034$. The time histories of displacement and velocity are presented in Figure 10 (a) and (b), respectively. The thin solid curves give the motion of the bottom and top oscillators. The thick solid curve depicts the motion of the particle. The shaded area indicates the region of stick motion, and the black circles represent the switching points of the motion. The particle with the top oscillator (P_4) impacts seven times, and the stick motion is formed with the top oscillator (P_6). The particle will free flight. The particle with the bottom oscillator impacts seven times (P_7). After that, the stick motion with the bottom oscillator (P_5) is formed. This forms a complete periodic motion. Discontinuity of the velocities can be observed from Figure 10 (b). The velocities of the bottom and top oscillators are very close to each other, and they do not change much after impact because the mass of the particle is much smaller than the two oscillators. The corresponding phase portrait of the particle with moving boundaries is presented in Figure 10 (c), where the thin solid curves indicate the moving boundaries, and the thick solid curve represents the motion of the particle. The discontinuity due to impacts is also observed from Figure 10 (c) for both of the moving boundaries and the motion of the particle. For illustration of the onset and vanishing condition of stick motion, the time histories of acceleration and jerk are presented in Figure 10 (d) and (e), respectively. After impacting seven times with the top oscillator, the velocities of particle and top oscillator become equal, and the acceleration of the top oscillator is less than the acceleration of the particle ($-g$), thus the onset conditions of stick motion with the top oscillator (P_6) are satisfied. Thus, the particle starts to move together with the top oscillator. This motion will continue until the forces per unit mass (or acceleration) equal to $-g$ again. At the same time, the jerks of the two become greater than zero, which satisfies the vanishing condition of stick motion on top. Thus, the motion relative to P_6 switches into the motion relative to P_2 . And then the particle impacts seven times with the bottom oscillator, until the velocity of the particle equals to that of the bottom oscillator, while at the same time, the acceleration of the bottom oscillator is greater than the one of the particle ($-g$); the onset condition of the stick motion on the bottom (P_5) satisfies. Thus, the particle starts moving together with the bottom oscillator until their acceleration equals to $-g$ again; mean while, their jerk is less than zero, which satisfies the vanishing condition of the stick motion on bottom. Thus the particle separates with the bottom oscillator and switches into the free flight motion in domain Ω_1 until the particle impacts with the top oscillator again.

The simulation of a chaotic motion is given in Figure 11 under the same parameters with $e = 0.9$. The initial conditions are $x_0^{(1)} = 0.941968193$, $\dot{x}_0^{(1)} = 1.86109613$, $x_0^{(2)} = 1.45709118$, $\dot{x}_0^{(2)} = 1.82722043$, $x_0^{(3)} = 1.45709118$, and $\dot{x}_0^{(3)} = 10.7134817$ for $t_0 = 0.289711605$. The time histories of displacements and velocities are presented in Figure 11 (a) and (b), respectively. The thin solid curves depict the motions of the bottom and top oscillators, and the thick solid curve represents the motion of particle. The switching sections for the particle, bottom and top oscillators in phase plane are also shown in Figure 11 (c) and (d), respectively. Furthermore, the switching sections for particle's displacement and velocity versus switching phase are presented in Figure 11 (e) and (f), respectively. The invariant set of such a chaotic motion is presented.





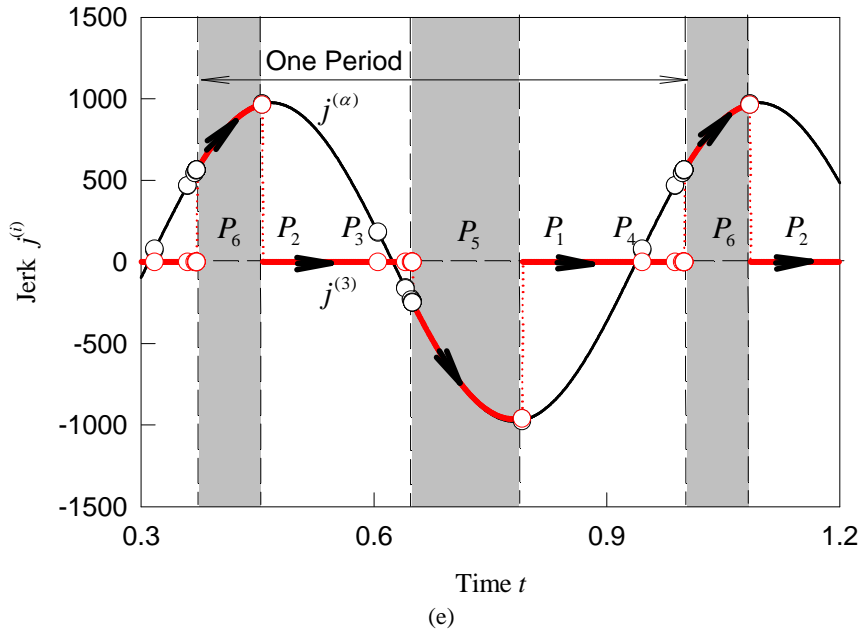
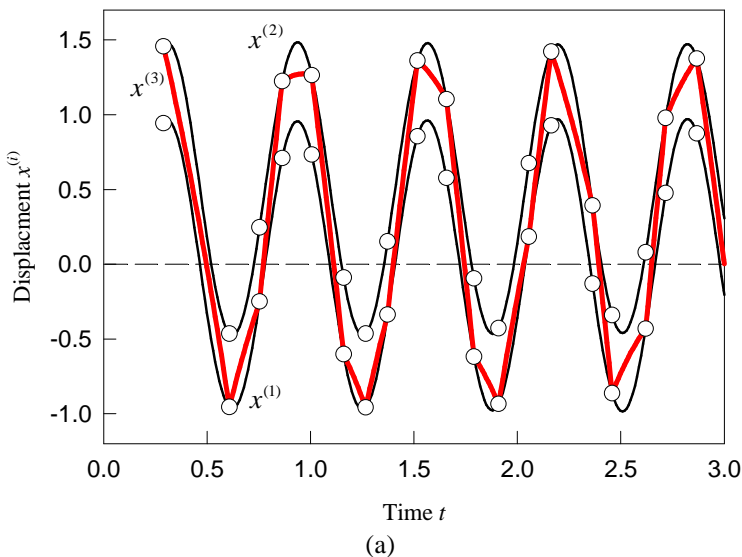
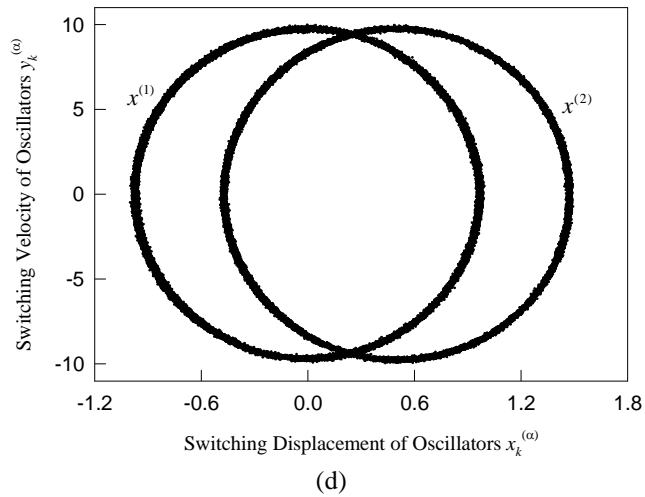
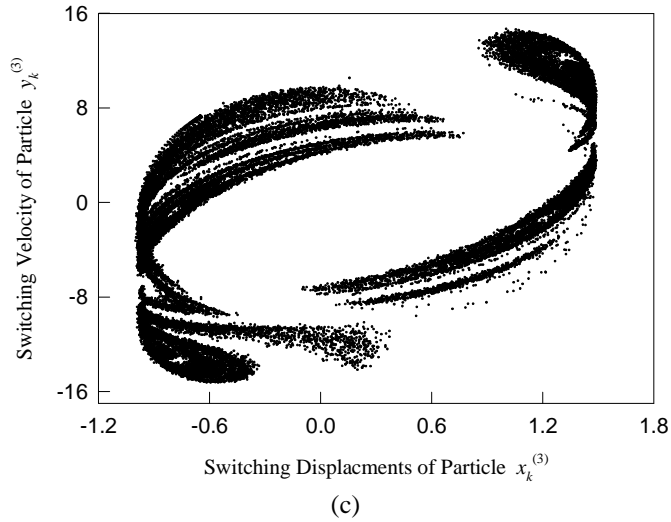
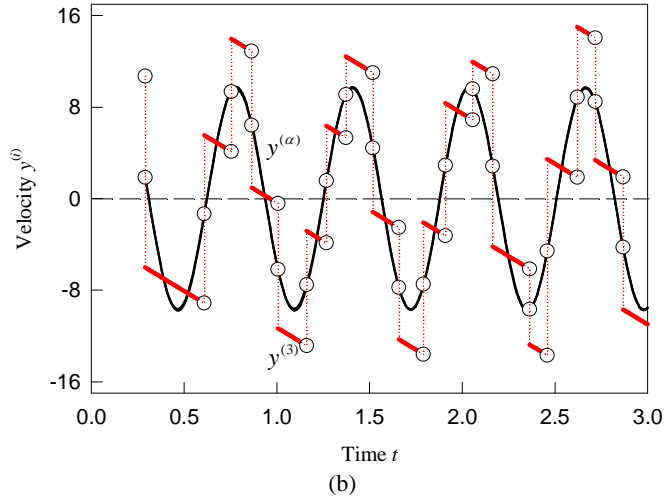
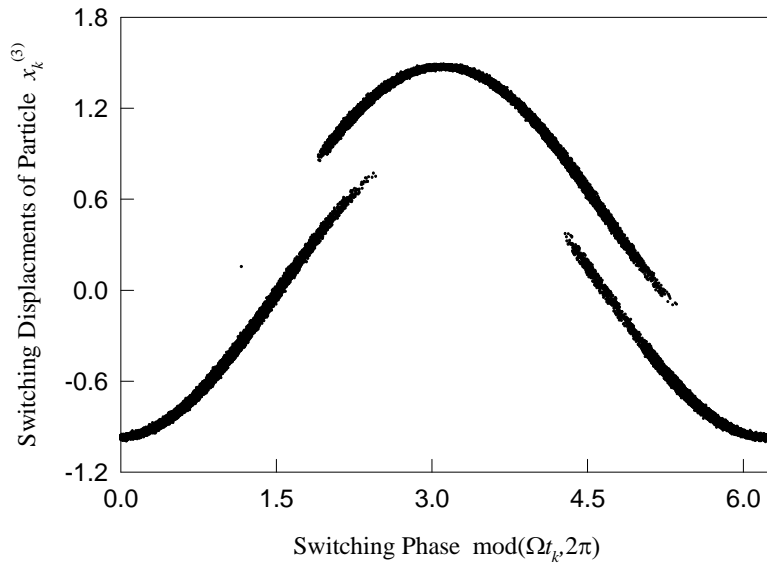


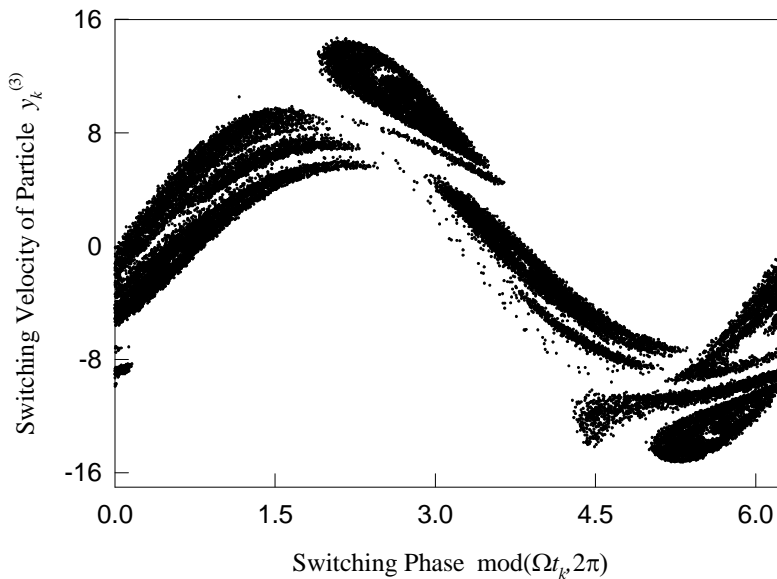
Fig. 10. Periodic motion with a mapping structure of $P_{253^7 164^7}$: (a) time history of displacement, (b) time history of velocity, and (c) a trajectory of particle with moving boundaries. $Q^{(1)} = Q^{(2)} = 20.0$, $\Omega^{(1)} = \Omega^{(2)} = 10.0$, $m^{(1)} = m^{(2)} = 1.0$, $m^{(3)} = 0.01$, $e^{(1)} = e^{(2)} = 0.2$, $h = 0.5$, $k^{(1)} = k^{(2)} = 80.0$, $c^{(1)} = c^{(2)} = 0.1$). The initial conditions are $x_0^{(1)} = 0.79534917$, $\dot{x}_0^{(1)} = -5.49025226$, $x_0^{(2)} = 1.30373854$, $\dot{x}_0^{(2)} = -5.51085936$, $x_0^{(3)} = 1.30373854$ and $\dot{x}_0^{(3)} = -5.57828916$ for $t_0 = 0.368919034$







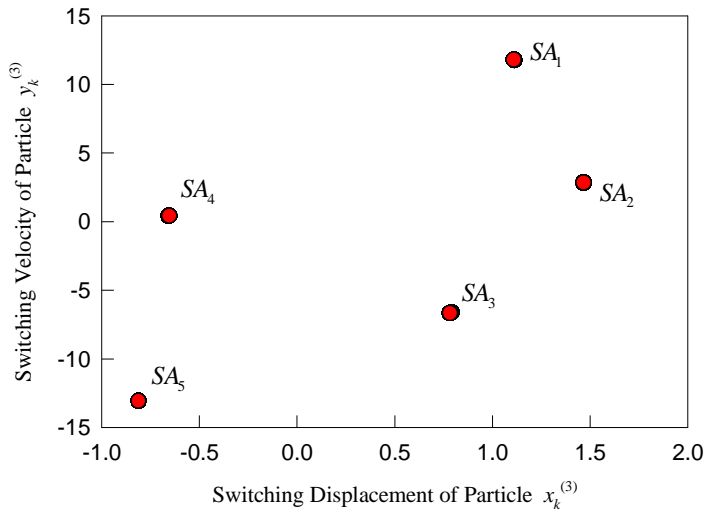
(e)



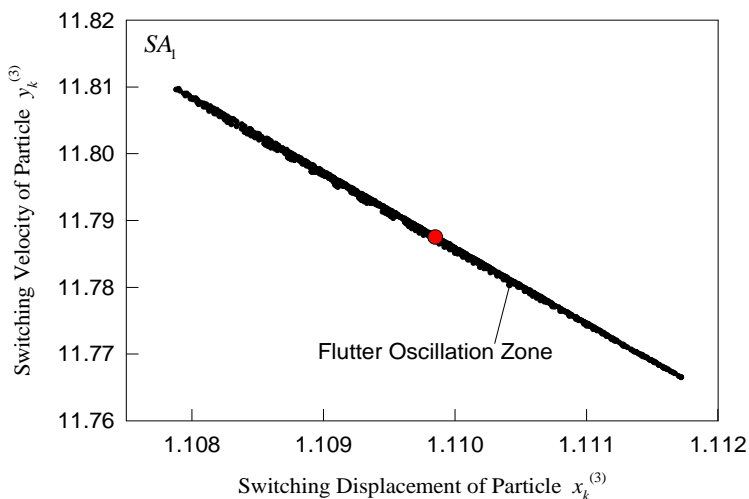
(f)

Fig. 11. Chaotic motion: (a) time history of displacement, (b) time history of velocity, (c) switching sections of $(x_k^{(3)}, y_k^{(3)})$, (d) switching sections of $(x_k^{(\alpha)}, y_k^{(\alpha)})$, (e) switching section of $(x_k^{(3)}, \text{mod}(\Omega t_k, 2\pi))$, and (f) switching section of $(y_k^{(3)}, \text{mod}(\Omega t_k, 2\pi))$. ($Q^{(1)} = Q^{(2)} = 20.0$, $\Omega^{(1)} = \Omega^{(2)} = 10.0$, $m^{(1)} = m^{(2)} = 1.0$, $m^{(3)} = 0.01$, $e = 0.9$, $h = 0.5$, $k^{(1)} = k^{(2)} = 80.0$, $c^{(1)} = c^{(2)} = 0.1$). The initial conditions are $x_0^{(1)} = 0.941968193$, $\dot{x}_0^{(1)} = 1.86109613$, $x_0^{(2)} = 1.45709118$, $\dot{x}_0^{(2)} = 1.82722043$, $x_0^{(3)} = 1.45709118$, and $\dot{x}_0^{(3)} = 10.7134817$ for $t_0 = 0.289711605$

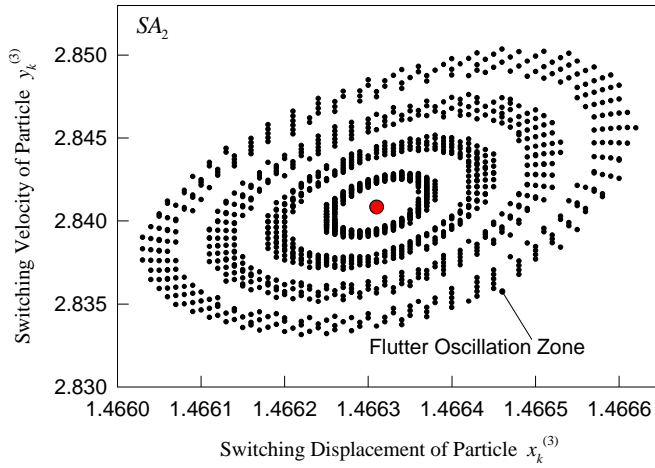
Two Neimark bifurcations with $e = 0.9067$ and $e = 1.0$ coexist with chaotic motions. The two Neimark bifurcations have five strange attractors with a very small scale of 10^{-3} . To illustrate the Neimark bifurcations, switching sections of the Neimark bifurcation with $e = 0.9067$ are carried out as shown in Figure 12. The input data for initial conditions of the simulation are listed in Table 1, and the center locations of each of the five strange attractors are listed in Table 2. The overall view of the five strange attractors of the Neimark bifurcation is presented in Figure 12 (a). The acronyms SA_i indicates the i th strange attractor with $i = 1, 2, \dots, 5$. A zoomed view of each strange attractor in Poincare mapping sections is then presented in Figure 12 (b)-(f), respectively. The flutter oscillation zone can be observed from each of the zoomed plots.



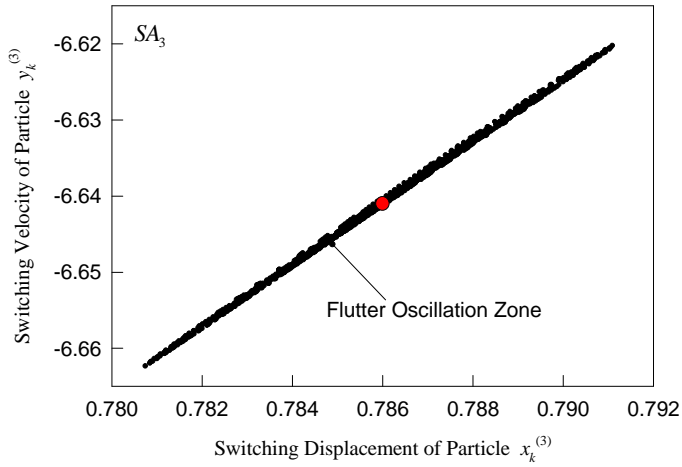
(a)



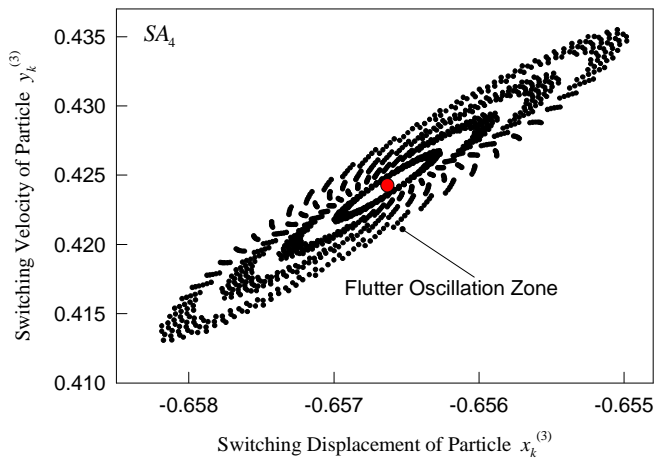
(b)



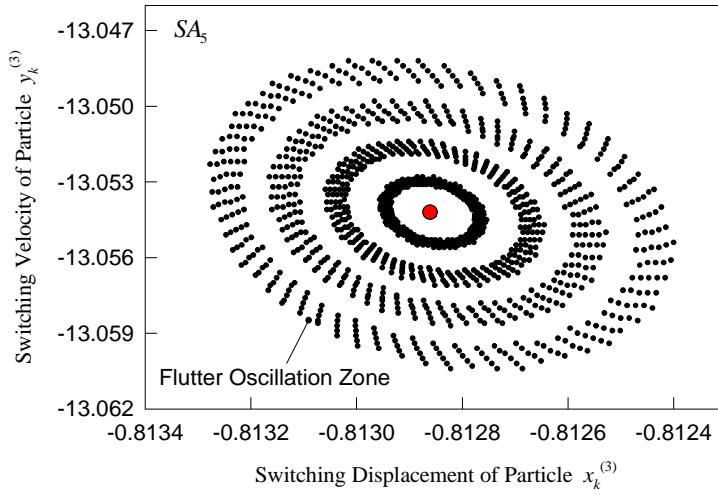
(c)



(d)



(e)



(f)

Fig. 12. Switching sections for the Neimark bifurcation of particle at $e = 0.9067$: (a) global view and (b)-(f) local view (SA_1 , SA_2 , SA_3 , SA_4 , and SA_5) ($Q^{(1)} = Q^{(2)} = 20.0$, $\Omega^{(1)} = \Omega^{(2)} = 10.0$, $m^{(1)} = m^{(2)} = 1.0$, $m^{(3)} = 0.01$, $h = 0.5$, $k^{(1)} = k^{(2)} = 80.0$, $c^{(1)} = c^{(2)} = 0.1$)

Table 1. Input data for switching sections of the Neimark bifurcation

(x_k, y_k)	(x_k, y_k)
$(-0.812857, -13.0542)$	$(-0.813146, -13.0542)$
$(-0.812946, -13.0542)$	$(-0.813217, -13.0542)$
$(-0.813038, -13.0542)$	

Table 2. Center location of each strange attractor

Strange Attractors	Center Locations (x_k, y_k)
SA_1	$(1.1098, 11.7877)$
SA_2	$(1.4663, 2.8409)$
SA_3	$(0.7860, -6.6410)$
SA_4	$(-0.6566, 0.4242)$
SA_5	$(-0.8129, -13.0542)$

Conclusions

The analytical conditions for stick and grazing motions to the boundaries for the Fermi oscillator with dual excitations were obtained analytically. The generic mappings are introduced to describe the periodic and chaotic motions. Bifurcation scenarios are presented numerically, and the analytical predictions of the stable and unstable periodic motions with certain mapping structures were also completed by eigenvalues stability analysis. Then, numerical illustrations of periodic and chaotic motions in such oscillators were given. The switching section for Neimark bifurcations was illustrated.

References

- [1] **Fermi E.** 1949, "On the origin of the cosmic radiation", *Physical review*, 75(8), pp. 1169-1174.
- [2] **Zaslavskii G. M. and Chirikov B. V.** 1964, "Fermi acceleration mechanism in the one-dimensional case", *Doklady Akademii Nauk SSSR*, 159, pp. 306-309.
- [3] **Holmes P. J.** 1982, "The dynamics of repeated impacts with a sinusoidally vibrating table", *Journal of Sound and Vibration*, 84, 173-189.
- [4] **Shaw S. W. and Holmes P. J.** 1983, "A periodically forced piecewise linear oscillator", *Journal of Sound and Vibration*, 90, pp. 129-155.
- [5] **Bapat C. N. and Popplewell N.** 1983, "Stable periodic motions of an impact-pair", *Journal of Sound and Vibration*, 87, pp. 19-40.
- [6] **Bapat C. N.** 1988, "Impact-pair under periodic excitation", *Journal of Sound and Vibration*, 120, pp. 53-61.
- [7] **Bapat C. N.** 1995, "The general motion of an inclined impact damper with friction", *Journal of Sound and Vibration*, 184, pp. 417-427.
- [8] **Luo A. C. J. and Han R. P. S.** 1996, "The dynamics of a bouncing ball with a sinusoidally vibrating table revisited", *Nonlinear Dynamics*, 10, pp. 1-18.
- [9] **Luna-Acosta G. A.** 1989, "Regular and chaotic dynamics of the damped Fermi accelerator", *Physical Review A*, 42, pp. 7155-7162.
- [10] **Lopac V. and Dananic V.** 1998, "Energy conservation and chaos in the gravitationally driven Fermi oscillator", *American Association of Physics Teachers*, 66, pp. 892-902.
- [11] **Saif F., Bialynicki-Birula I., Fortunato M. and Schleich W. P.** 1998. "Fermi accelerator in atom optics", *Physical Review A*, 58, pp. 4779-4783.
- [12] **Bouchet F.** 2004, "Minimal stochastic model for Fermi's acceleration", *Physical Review Letters*, 92(4), 040601(1-4).
- [13] **Leonel E. D., da Silva J. K. L. and Kamphorst S. O.** 2004, "On the dynamical properties of a Fermi accelerator model", *Physica A*, 331, pp. 435-447.
- [14] **Leonel E. D. and McClintock P. V. E.** 2005, "A hybrid Fermi-Ulam-bouncer model", *Journal of Physics A: Mathematical and General*, 38, pp. 823-839.
- [15] **Leonel E. D., de Carvalho R. E.** 2006, "A family of crisis in a dissipative Fermi accelerator model", *Physics Letters A*, 364, pp. 475-479.
- [16] **Leonel E. D. and Silva M. R.** 2008, "A bouncing ball model with two nonlinearities: a prototype for Fermi acceleration", *Journal of Physics A: Mathematical and Theoretical*, 41, Article ID 015104.
- [17] **Luo A. C. J.** 2002, "An unsymmetrical motion in a horizontal impact oscillator", *Journal of Vibration and Acoustics*, 124, pp. 420-426.
- [18] **Giusepponi S., Marchesoni F., Borromeo M.** 2004, "Randomness in the bouncing ball dynamics", *Physica A*, 351, pp. 143-158.
- [19] **Luo A. C. J.** 2005, "The mapping dynamics of periodic motions for a three-piecewise linear system under a periodic excitation", *Journal of Sound and Vibration*, 283, pp. 723-748.
- [20] **Luo A. C. J.** 2005, "A theory for non-smooth dynamic systems on the connectable domains", *Communications in Nonlinear Science and Numerical Simulation*, 10, pp. 1-55.

- [21] **Luo A. C. J. and Chen L.** 2005, "Grazing bifurcation and periodic motion switching in a piecewise linear, impacting oscillator under a periodical excitation", *American Society of Mechanical Engineers, Design Engineering Division*, DE 118 B (2), pp. 913-924.
- [22] **Luo A. C. J. and Gegg B. C.** 2006, "Stick and non-stick periodic motions in periodically forced oscillators with dry friction", *Journal of Sound and Vibration*, 291, pp. 132-168.
- [23] **Luo A. C. J. and O'Connor D.** 2007, "Mechanism of impacting chatter with stick in a gear transmission system", *International Journal of Bifurcation*, 19(6), pp. 2093-2105.
- [24] **Luo A. C. J. and O'Connor D.** 2007, "Periodic motion and chaos with impacting chatter and stick in a gear transmission system", *International Journal of Bifurcation*, 19(6), pp. 1975-1994.
- [25] **Luo A. C. J.** 2008, Global Transversality, Resonance and Chaotic Dynamics, *World Scientific: Singapore*.
- [26] **Luo A. C. J. and Guo Y.** 2009, "Motion switching and chaos of a particle in a generalized Fermi-acceleration oscillator", *Mathematical Problems in Engineering*, Article ID 298906, pp.1-40.
- [27] **Luo A. C. J. and Guo Y.** 2010, "Switching mechanism and complex motions in an extended Fermi-acceleration oscillator", *Journal of Computational and Nonlinear Dynamics*, 5(4), pp. 1-14
- [28] **Luo A. C. J. and Guo Y.** 2010, "Switchability and bifurcation of motions in a double-excited Fermi-acceleration oscillator", *Proceedings of the 2010 ASME International Mechanical Engineering Congress and Exposition*, IMECE2010-39165.
- [29] **Luo A. C. J.** 2008, A theory for flow switchability in discontinuous dynamical systems, *Nonlinear Analysis: Hybrid Systems*, 2(4), pp.1030-1061.
- [30] **Luo A. C. J.** 2009, Discontinuous Dynamical Systems on Time-varying Domains, HEP-Springer: Dordrecht.